AD_____

Award Number: DAMD17-98-1-8121

TITLE: Ultrasonic Stimulated Acoustic Emission for Detection of Breast Microcalcifications

PRINCIPAL INVESTIGATOR: Mostafa Fatemi, Ph.D.

CONTRACTING ORGANIZATION: Mayo Foundation
Rochester, Minnesota 55905

REPORT DATE: May 2001

TYPE OF REPORT: Annual

PREPARED FOR: U.S. Army Medical Research and Materiel Command
Fort Detrick, Maryland 21702-5012

REPORT DOCUMENTATION PAGE

Form Approved
OMB No. 074-0188

1. AGENCY USE ONLY (Leave blank)	2. REPORT DATE	3. REPORT TYPE AND DATES COVERED
	May 2001	Annual (15 Apr 00 - 14 Apr 01)

4. TITLE AND SUBTITLE
Ultrasonic Stimulated Acoustic Emission for Detection of Breast Microcalcifications

5. FUNDING NUMBERS
DAMD17-98-1-8121

6. AUTHOR(S)
Mostafa Fatemi, Ph.D.

7. PERFORMING ORGANIZATION NAME(S) AND ADDRESS(ES)
Mayo Foundation
Rochester, Minnesota 55905

E-Mail: fatemi.mostafa@mayo.edu

8. PERFORMING ORGANIZATION REPORT NUMBER

9. SPONSORING / MONITORING AGENCY NAME(S) AND ADDRESS(ES)
U.S. Army Medical Research and Materiel Command
Fort Detrick, Maryland 21702-5012

10. SPONSORING / MONITORING AGENCY REPORT NUMBER

11. SUPPLEMENTARY NOTES
This report contains colored photos

12a. DISTRIBUTION / AVAILABILITY STATEMENT
Approved for Public Release; Distribution Unlimited

12b. DISTRIBUTION CODE

13. ABSTRACT *(Maximum 200 Words)*

The **purpose** of this research is to develop an experimental imaging system based on Ultrasound Stimulated Acoustic Emission (USAE) for detecting microcalcifications in human breast tissue specimens. The **scope** of this research is to improve the laboratory USAE system and evaluate its performance on breast tissue specimens containing microcalcifications. The first task of this research is focused on system development and optimization for detection of beast microcalcifications. The second task is centered on imaging breast tissues and evaluating the performance of USAE method in detection of microcalcifications. Here we report our progress on imaging tissue samples (Task 2). **Results** show that USAE can detect microcalcifications in various pathological conditions. We also report recent improvements in our experimental system.

14. SUBJECT TERMS	15. NUMBER OF PAGES
Breast Cancer, Microcalcification, Ultrasound, Acoustic Emission	51
	16. PRICE CODE

17. SECURITY CLASSIFICATION OF REPORT	18. SECURITY CLASSIFICATION OF THIS PAGE	19. SECURITY CLASSIFICATION OF ABSTRACT	20. LIMITATION OF ABSTRACT
Unclassified	Unclassified	Unclassified	Unlimited

FOREWORD

Opinions, interpretations, conclusions and recommendations are those of the author and are not necessarily endorsed by the U.S. Army.

___ Where copyrighted material is quoted, permission has been obtained to use such material.

___ Where material from documents designated for limited distribution is quoted, permission has been obtained to use the material.

__X__ Citations of commercial organizations and trade names in this report do not constitute an official Department of Army endorsement or approval of the products or services of these organizations.

N/A In conducting research using animals, the investigator(s) adhered to the "Guide for the Care and Use of Laboratory Animals," prepared by the Committee on Care and use of Laboratory Animals of the Institute of Laboratory Resources, national Research Council (NIH Publication No. 86-23, Revised 1985).

X For the protection of human subjects, the investigator(s) adhered to policies of applicable Federal Law 45 CFR 46.

N/A In conducting research utilizing recombinant DNA technology, the investigator(s) adhered to current guidelines promulgated by the National Institutes of Health.

N/A In the conduct of research utilizing recombinant DNA, the investigator(s) adhered to the NIH Guidelines for Research Involving Recombinant DNA Molecules.

N/A In the conduct of research involving hazardous organisms, the investigator(s) adhered to the CDC-NIH Guide for Biosafety in Microbiological and Biomedical Laboratories.

Mostafa Fatemi 6/13/01

PI - Signature Date

TABLE OF CONTENTS

1. INTRODUCTION

The vision of this research is to develop a new non-invasive imaging modality for breast imaging that is capable of detecting small microcalcifications. Our present goal is to further develop an experimental system based on Ultrasound Stimulated Acoustic Emission (USAE) for in vitro imaging of breast tissue specimens and test its performance in detecting microcalcification. The general theory of USAE is described in [1-3], and some of its applications are explained in [3,4].

The first task of this research is focused on system development and optimization for detection of beast microcalcification. The second task, covering the second and third year, is centered on tissue imaging. This report addresses the activities related to Task 2 of the project. We also report new developments in our continued effort to improve our experimental system and image quality.

2. BODY

2.1. Tissue Experiments

This activity relates to Task 2 of the proposal. We continued imaging more breast tissues during the past year. USAE images were compared to the corresponding x-ray mammography images. Results of these two imaging modalities are generally in agreement. We also studied the histology of some specimens and microcalcifications. Table 1. Describes the results.

Table 1. Histological evaluation of breast tissue specimens

Specimen	Histology	Calcification
1	Invasive lobular carcinoma, proliferative breast disease	Calcifications in cysts, apocrine metaplasia and fibroadenomatous nodules
2	Invasive lobular carcinoma, proliferative breast disease	Calcifications in fibroadenomatous hyperplasia
3	Proliferative breast disease	Calcifications in sclerosing adenosis
4	Proliferative breast disease	Calcifications in apocrine metaplasia and fibrosis
5	Proliferative breast disease	Calcifications in sclerosing adenosis
6	Proliferative breast disease	Calcifications in apocrine metaplasia and sclerosing adenosis
7	Proliferative breast disease	Calcifications in ductal hyperplasia and apocrine metaplasia
8	Atypical lobular hyperplasia	Calcifications in hyperplastic lobules

9	Ductal carcinoma in situ, comedo type	Calcifications in comedo necrosis
10	Ductal carcinoma in situ, comedo type	Calcifications in comedo necrosis
11	Fibrosis	A Calcification in fibrosis
12	Proliferative breast disease	Calcifications in cysts
13	Proliferative breast disease	Calcifications in ductal hyperplasis
14	Proliferative breast disease	Calcifications in cysts
15	Proliferative breast disease	Calcifications in cysts
16	Proliferative breast disease	Calcifications in sclerosing adenosis

Examples of USAE images of some tissue specimens are shown in Figs. 1 and 2. For more detail refer to [5,6].
There are several factors that limit the performance of USAE in detecting microcalcifications. Because microcalcifications are very small objects, they produce a weak acoustic emission field. Detection of such a weak acoustic field is often a challenging task. We have improved the signal-to-noise ratio of the receiver by employing a phase-locked receiver in our system (described in the next sub-section). Another limiting factor is the standing wave in the water tank. Establishment of the standing wave in the experiment water tank may cause the sensitivity of the imaging system to become a function of object and hydrophone positions. Introducing acoustic absorbers in the water tank has reduced the effect of standing waves.

2.2. System Development

During the past year we continued our effort to improve different aspects of the experimental USAE system. Some of these activities are listed below.

2.2.1. Receiver Lock-in Amplifier

Our previous receiver included a per-amplifier followed by a narrow-band programmable filter. This configuration operates well as long as the signal level at the hydrophone is high enough for subsequent amplification and detection. However, when imaging small microcalcifications, the signal level can be very low in comparison to the ambient noise within the pass-band of the narrow-band filter. Figure 3 shows the simplified diagram of this system. There are several sources of noise in the system, including airborne noise in the room, structural vibrations, acoustic noise from the scanning motors, and the noise from equipment fans. There is also some electrical noise in the system.

To improve the signal-to-noise ratio, we modified the receiver by replacing the preamplifier and the programmable filter with a lock-in amplifier (EG&G Instruments, Model 7264 DSP). The lock-in amplifier uses a reference signal to set the lock frequency. The frequency of the reference signal must be exactly equal to the frequency of the input signal to the amplifier (hydrophone output). This system locks to the frequency of the reference signal ($\Delta\omega$) and tracks the input signal by an active phase-lock loop. In effect, the lock-in amplifier acts as a very narrow band filter with a pass band of only a few Hz centered at the difference frequency $\Delta\omega$. This system allows the acoustic emission signal to pass and rejects the noise outside the pass band. The reference signal (at $\Delta\omega$) is provided by down-mixing the signals from the two RF generators driving the two elements of the transducer. The simplified diagram of the new system is shown in Figure 4.

2.2.2. Improved System Control:

To improve the scanning process a GPIB control card has been added to the scanner workstation (Sun Sparc Station 5). This card allows all sub-systems, such as RF generators, lock-in amplifier, digitizer, and the new scanner system with servomotors, to be controlled by software. This system operates under LabView software.

2.2.3 Interactive Imaging and Object Analysis

New software has been developed for interactive scanning and data collection. An important feature of the new software is its capability to produce the image of the object as it is scanned, and allows the user to select a point on the image and reposition the transducer beam to the selected points in the object. Once at the new position, the system can collect the acoustic emission signal from that particular point of the object.

Another important feature of this software is its capability in measuring the frequency response of a selected point in the object. This feature allows the user to point the ultrasound beam at a selected point in the object and sweep the vibration frequency $\Delta\omega$ while the system records the acoustic emission signal. Employing a built-in fast Fourier transform algorithm, this system then calculates and displays the frequency response (spectrum) of the object. This feature is particularly useful in imaging and analyzing the frequency response of microcalcifications. We hope that the frequency domain signature would help us to differentiate different types of microcalcifications in breast tissue. This would open the way for using USAE as a characterization tool, or "noninvasive biopsy", in future.

2.2.4. Anechoic chamber:

Because USAE experiments are performed at low acoustic intensities, it is essential to keep the environmental noise and structural vibration as low as possible. For this purpose, we have designed a 12'x10'x7' anechoic chamber (quiet room) with a 150 Hz cutoff frequency. This room includes acoustically insulated walls and floor, with the interior covered with absorbing wedges. Our future tissue experiments will take place in this room. We expect that using this room will significantly reduce the noise level and improve the quality of data in our experiment. Funding for the anechoic chamber is

provided by a Major Research Instrumentation grant from the National Science Foundation. Mayo Clinic provides the space for this room.

2.2.5. Scanning Vibrometer

The main function of USAE is to vibrate the object by the radiation force of ultrasound. It is therefore a fundamental issue to understand object vibration and its role in generating the acoustic emission field. In order to analyze object vibration and verify our acoustic measurements we need to measure such vibrations directly. For this purpose we have acquired a scanning vibrometer (Polytec VibraScan PSV-300F) that enables us to measure object vibrations in two dimensions, in Angstrom range, and produce an image (or a movie) that shows displacement (or particle velocity) at every point on the objet. (This instrument is in addition to the laser vibrometer reported last year, which measures vibration at only one point at a time.) This tool will help us to further develop USAE for breast imaging. The funds or this instrument is provided by a Major Research Instrumentation grant from the National Science Foundation.

2.3. Theoretical Developments

In an effort to better understand the response of microcalcification in response to the radiation force of ultrasound we have modeled microcalcification as an elastic sphere in a fluid medium. The sphere is exposed to two plane ultrasound waves at slightly different frequencies. The vibration velocity of the sphere and the acoustic emission field has been calculated in terms of sphere size and elastic properties. Experiments on steel spheres were carried out and the velocity of the sphere was measured directly by a laser interferometer system (vibrometer). We also measured the acoustic emission field by a calibrated hydrophone. The experimental result supports the model. For more detail refer to reference [7]. This theory will be useful in quantitative analysis of microcalcification using USAE.

2.4. Discussion

The histology of the tissue samples indicates that USAE can image breast microcalcifications in a wide range of pathological conditions (Tab. 1.). This improves our prospects for future use of USAE for in-vivo breast imaging. In most cases tissue inhomogenieties seem not to interfere with detection of microcalcifications. We are planning to continue to image a larger number of tissue specimens with various types of calcifications. This will help us to better assess the performance of USAE under different conditions. Also, we are planning to study in more depth the effect of different tissue inhomogenieties on USAE images.

3. Key Research Accomplishments

- Demonstrated that small microcalcification can be detected by USAE imaging method.
- Demonstrated that USAE can detect microcalcifications in various pathological conditions.
- We have shown that using a lock-in amplifier as the first stage of the receiver can increase the sensitivity of the system and improve the signal-to-noise ratio of the resulting images.

4. Reportable Outcomes

1. Fatemi, M, Wold, LE, Alizad, A, and Greenleaf JF, Vibro-acoustic tissue mammography. IEEE Trans. on Med. Imag., 2001 (submitted).
2. Fatemi, M, and Greenleaf JF, Imaging and evaluating the elastic properties of biological tissues. BMUS Bulletin, 8(4):16-18, Nov. 2000.
3. Fatemi, M, Wold, LE, Morton, MJ, and Greenleaf, JF, Imaging Breast microcalcifications by vibro-acoustography. J Ultrasound Med. 20(3): S25-26, 2001.
4. Fatemi, M and Greenleaf, JF, New trends in ultrasonic imaging, 2000 IEEE Solid-State Circuits and Technology Committee Workshop on Biomedical Electronics (B. Ziaie and J. Von Arx), Oct. 2000 (Invited presentation).
5. Chen, S, Fatemi, M, and Greenleaf, JF: Vibro-acoustography of Small Spheres. J Acoust Soc Am 108(5 pt. 2): 2505, November 2000.
6. Army Medical Research, BCRP, Idea Award: Development of vibro-acoustography for in-vivo detection of breast microcalcifications. Proposal submitted June 2001.
7. NIH, Award Program PAR-01-057 (Technology Development for Biomedical Applications Program): Vibro-acoustography system with contact array probe. Proposal submitted May 2001.

5. Conclusions

Our experimental results thus far indicate that microcalcifications in various pathologic conditions can be detected by USAE imaging. Image quality and system sensitivity is improved by using a lock-in amplifier to track the frequency of the low-level acoustic emission signal.

5.1. So What?

The body of knowledge collected in this research may be used to development of a new class of non-invasive imaging tool for breast imaging and visualization of breast microcalcifications. Two grant applications for the development of such in-vivo USAE imaging system has been submitted to the Federal agencies (see Army BCRP and NIH grant proposals, Appendices 6 and 7).

6. References

1. Fatemi M, and Greenleaf, JF, "Vibro-acoustography. An imaging modality based on ultrasound stimulated acoustic emission," Proc. Nat. Acad. Sci. USA., vol. 96, pp. 6603-6608, June 1999.

2. Fatemi, M., and Greenleaf, JF: Ultrasound-stimulated vibro-acoustic spectrography. Science 280:82--85, April 3, 1998.

3. Fatemi, M, and Greenleaf, JF, "Probing the dynamics of tissue at low frequencies with the radiation force of ultrasound," Phys. Med. Biol., vol. 45, pp.1449-1464, 2000.

4. Fatemi, M, and Greenleaf JF, Imaging and evaluating the elastic properties of biological tissues. British Medical Ultrasound (BMUS) Bulletin, 8(4):16-18, Nov. 2000.

5. Fatemi, M. Wold, LE, Morton, MJ, and Greenleaf, JF, Imaging Breast microcalcifications by vibro-acoustography. J Ultrasound Med. 20(3): S25-26, 2001.

6. Fatemi, M, Wold, LE, Alizad, A, and Greenleaf JF, Vibro-acoustic tissue mammography. IEEE Trans. on Med. Imag., 2001 (submitted).

7. Chen, S, Fatemi, M, and Greenleaf, JF: Vibro-acoustography of Small Spheres. J Acoust Soc Am 108(5 pt. 2): 2505, November 2000.

7. Appendices

Appendix 1: Figures and legends (page... of this report)

Appendix 2: Fatemi, M, Wold, LE, Alizad, A, and Greenleaf JF, Vibro-acoustic tissue mammography. IEEE Trans. on Med. Imag., 2001 (submitted). (page... of this report).

Appendix 3: Fatemi, M, and Greenleaf JF, Imaging and evaluating the elastic properties of biological tissues. BMUS Bulletin, 8(4):16-18, Nov. 2000. (page... of this report)

Appendix 4: Fatemi, M, Wold, LE, Morton, MJ, and Greenleaf, JF, Imaging Breast microcalcifications by vibro-acoustography. J Ultrasound Med. 20(3): S25-26, 2001. (page... of this report)

Appendix 5: Chen, S, Fatemi, M, and Greenleaf, JF: Vibro-acoustography of Small Spheres. J Acoust Soc Am 108(5 pt. 2): 2505, November 2000. (page... of this report)

Appendix 6: Army Medical Research, BCRP, Idea Award proposal: Development of vibro-acoustography for in-vivo detection of breast microcalcifications. Proposal submitted June 2001. (page... of this report)

Appendix 7: NIH, Award Program PAR-01-057 grant proposal (Technology Development for Biomedical Applications Program): Vibro-acoustography system with contact array probe. Proposal submitted May 2001. (page... of this report)

Appendix A

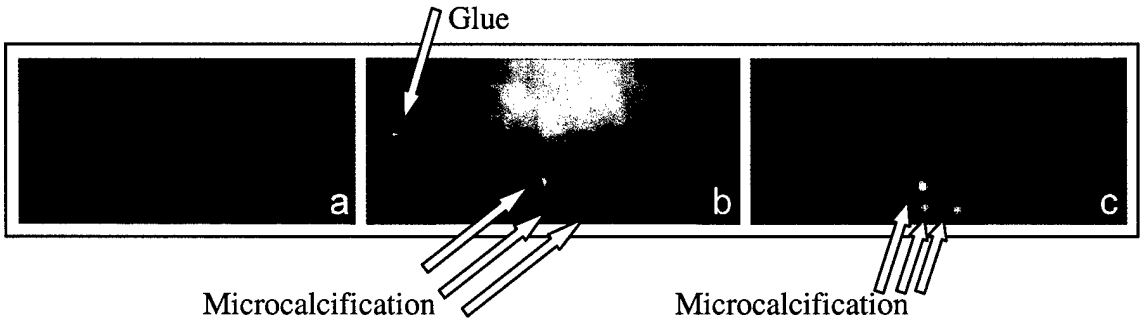

Figure 1. USAE image of a breast specimen. (a) Photograph of the tissue specimen mounted on the scanning bracket. (b) X-ray mammography of (a), showing some MCs at the center of the image. (c) Vibro-acoustography of (a). MCs can be seen as bright spots at same location as in the x-ray. (A glue droplet, whish is used to bond the tissue to the latex sheet, is seen on the left side of the tissue)

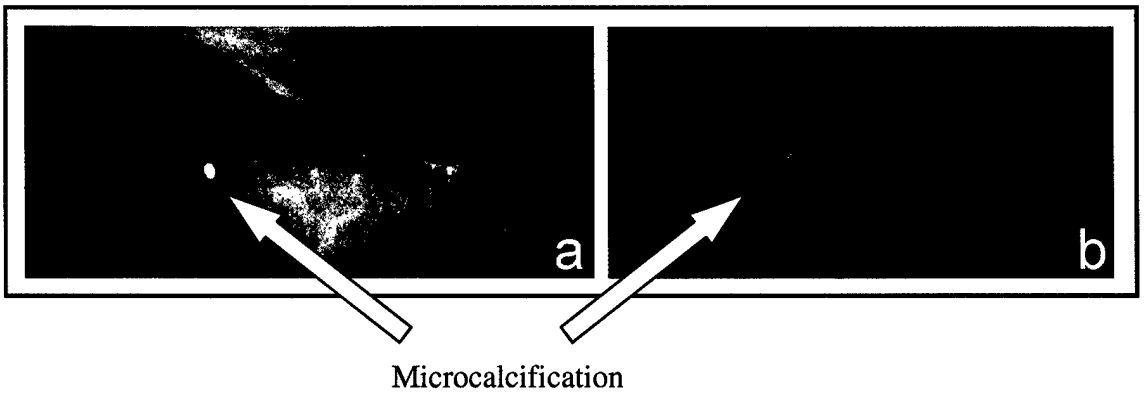

Figure 2. USAE of a breast tissue sample. (a) X-ray image indicating the existence of a microcalcification in the tissue. (b) USAE image obtained at the difference frequency Δf= 22 kHz. The microcalcification can be seen in this image.

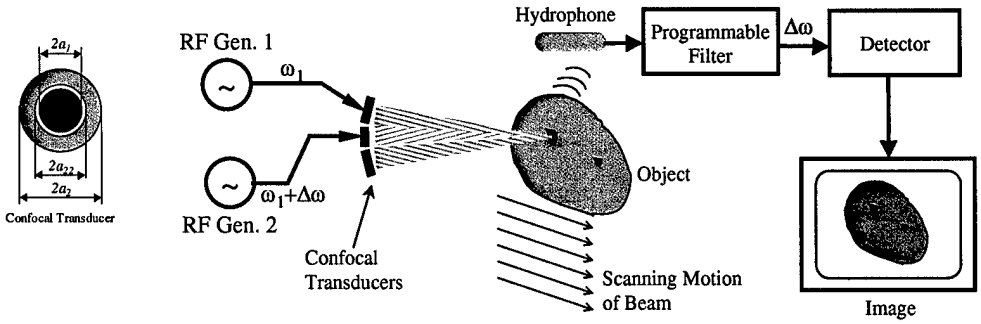

Figure 3. Simplified diagram of the USAE imaging system with a programmable filter. The bandpass filter tuned to the frequency of the acoustic emission signal (Δω).

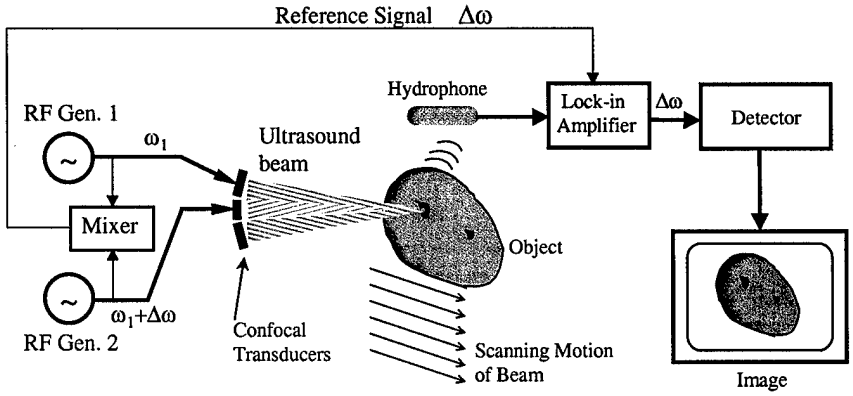

Figure 4. Simplified diagram of the USAE imaging system with a lock-in amplifier. The reference signal is obtained by down mixing the driving signals of the transducer. The lock-in amplifier locks to the frequency of the reference signal to allow only Δω component of the hydrophone signal to pass through.

Imaging and Evaluating the Elastic Properties of Biological Tissues

M Fatemi, JF Greenleaf

Department of Physiology and Biophysics, Mayo Clinic and Mayo Foundation, Rochester, MN, USA

Introduction

A common approach for evaluating some of the characteristics of an object is listening to the sound that object makes. This approach is used for many purposes in our daily life. Evaluating the quality of a crystal glass by tapping a finger on it is a simple example. Plucking a violin string to adjust the tuning is another.

It is well known that changes in elasticity of soft tissues are often related to pathology. Physicians traditionally use sound as a diagnostic tool, for example, by tapping on the patient's body. Vibro-acoustography implements the same concept but in micro-scale, and in a way that can be applied to living tissues. This method uses a small point-like tapping force that vibrates a region within the body, while a sensitive microphone is used to listen to the "sound" of the vibrating region.

In analogy to the sound of the crystal glass, sound from the body carries some information about the structure and the material properties of the region in the body. For example, the loudness of the sound may indicate the hardness of the body region being vibrated. Also, regions with different elasticity may respond differently at different frequencies. Sound from body vibrations can be used to produce an image of the body. To do this, the point-like tapping force is moved across the region of interest in a raster motion, and the sound emitted from each point is used to determine the brightness of the corresponding point on the image display system. The result is a display of elastic properties of the region of interest.

In this paper, we first describe how vibro-acoustography works, then present results of some experiments on biological tissues.

Vibro-acoustography

Vibro-acoustography produces a map of the mechanical response of an object to a dynamic force applied at each point. The method utilizes ultrasound radiation force to remotely exert a localized force (a force that is confined to a small region) at a desired frequency within (or on the surface of) an object, and records the resultant acoustic response[1,2]. This acoustic response, which is normally at low kHz range, is a function of the viscoelastic properties of the object and can be used to produce an image of the object[3].

Before introducing the system, we shall briefly discuss the phenomenon of the radiation force. The phenomenon of acoustic radiation force and radiation pressure has been studied for a century[4,5]. The acoustic radiation force is an example of a universal phenomenon in any wave motion that introduces some type of unidirectional force on absorbing or reflecting targets in the wave path. For example, the radiation force of sunlight pushes the tail of comets away from the sun. Similarly, a sound wave can produce the radiation force on objects it interacts with. Vibro-acoustography utilizes an oscillating radiation force of ultrasound to vibrate the tissue, and consequently, produce an acoustic emission from the object. To produce an oscillating radiation force the intensity of the incident ultrasound must be amplitude modulated at the desired low frequencies. Using a single amplitude modulated beam seems to be the simplest means to attain this purpose. However, such a beam will exert a radiation force on any object that is present along the beam path, producing undesirable acoustic emission. To confine oscillations of the radiation stress to the desired region, vibro-acoustography uses two unmodulated continuous wave beams at slightly different frequencies, propagating along separate paths. The beams are arranged to cross each other at their respective foci, and thus produce a modulated field at a confined, small, cross over region. This beam produces a force, oscillating at the difference frequency, on any object located at the focal region.

Figure (1) illustrates a vibro-acoustography system. The elements of a two-element annular array transducer are driven by two continuous wave signals at frequencies f_1 and f_2. The object to be imaged is placed at the joint focal plane of the transducer elements (the scanning plane). The ultrasound field produces a localized radiation stress at the focal point on the object at frequency $f_2 - f_1$. Depending on the elastic properties of the object, the radiation force may cause a portion of the object, or the entire object, to vibrate at this frequency. The acoustic emission resulting from object vibration is received by a hydrophone (or microphone) that is located nearby. Normally, the wavelength of the vibration is large compared to the object size, hence the acoustic emission field is almost omnidirectional. Therefore, hydrophone position is not a critical parameter in this measurement. The filter is used to eliminate noise and other interfering signals. To form an image, the focal point of the transducer is moved across the scanning plane within the object in a raster pattern. The acoustic emission is received at each position, and an image is formed by displaying the amplitude (or phase) of such signals at corresponding positions on the image plane. The spatial resolution of this imaging method is determined by the ultrasound beamwidth at the focal plane, which is normally comparable to the incident ultrasound wavelength.

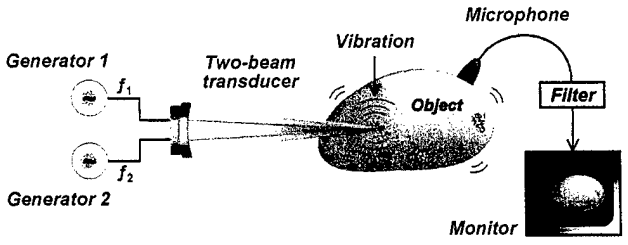

Fig. 1. Vibro-acoustography system. The object is vibrated by the radiation force of the confocal, two-beam transducer. Resulting vibrations are detected by the microphone (or hydrophone) and mapped into the image.

Experiments

In medical applications, one can use vibro-acoustography to obtain images of the human body for diagnostic purposes. To demonstrate the capability of vibro-acoustography, we used this method to image a specimen of human iliac artery that included calcifications. A 3 MHz transducer, with a diameter of 45mm and focal length of 70mm, was used for this experiment. The difference frequency was set at 44 kHz (this is also the frequency of object vibrations). Figure (2a) shows a photo of the artery that is cut open. The areas with calcification are marked

by letter "C". The vibro-acoustic image of the same artery is shown in Fig. (2b). Calcium deposits are formed in large plates, ranging in size from a few mm to a few cm. Such calcium plates, which are much stiffer than the arterial wall, constitute efficient acoustic radiators and can produce a strong acoustic field when vibrated by the radiation force of the incident ultrasound, allowing the calcified regions to stand out in the vibro-acoustography image.

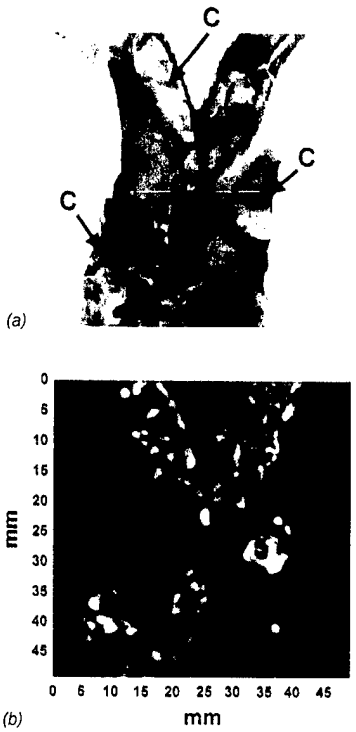

Fig. 2. Vibro-acoustic image of an ex-vivo human iliac artery near the bifurcation. On the left (a) is a photo of the cut-open artery specimen. Calcified areas are marked with letter "C". Vibro-acoustic image of the specimen is shown on the right (b). Calcified areas stand out as bright spots. This image was obtained with a 3 MHz confocal transducer as described in the text. The difference frequency was set at 44 kHz. The gray-level scale is in arbitrary units. (Reproduced with permission from Reference 6)

The next example illustrates detection of micro-calcifications in breast tissue. Figure (3a) shows a photograph of a piece of human breast tissue collected from a 57-year-old subject. Two small sutures are knotted on the tissue for identification purpose. Figure (3b) shows the x-ray mammogram of this tissue piece. The sutures are barely visible in this mammogram. This sample was scanned by a vibro-acoustography system similar to the one used in the previous experiment. The resulting vibro-acoustic image of the tissue at 25 kHz is shown in Fig. (3c). Micro-calcifications can be seen in this image as bright spots. It is interesting to note that the number and position of micro-calcifications matches with the corresponding spots in the x-ray mammogram. Also noticeable is that tissue inhomogeneities appear dim and do not interfere with calcification in the acoustic image. Sutures are also visible in the vibro-acoustic image, apparently because they contain entrapped gas.

The above experimental results show that vibro-acoustography can be used for high-quality imaging. The spatial resolution is comparable to the ultrasound beamwidth at the focal region. For example, for the 3 MHz ultrasound transducer used in the experiments, the spatial resolution is about 700 μm. These results also show that vibro-acoustic images have high signal-to-noise ratio and no speckle. These features allow vibro-acoustography to delineate calcium deposits with high definition and contrast.

In summary, elastic properties of tissue appear to be closely related to tissue pathology. These properties also relate to our perception of how the tissue feels. Therefore, they are readily understandable by the physician. The value of the information on elastic properties of tissue cannot be overemphasized. Methods aimed at imaging or evaluating elastic features of tissue promise a new era in diagnostic imaging.

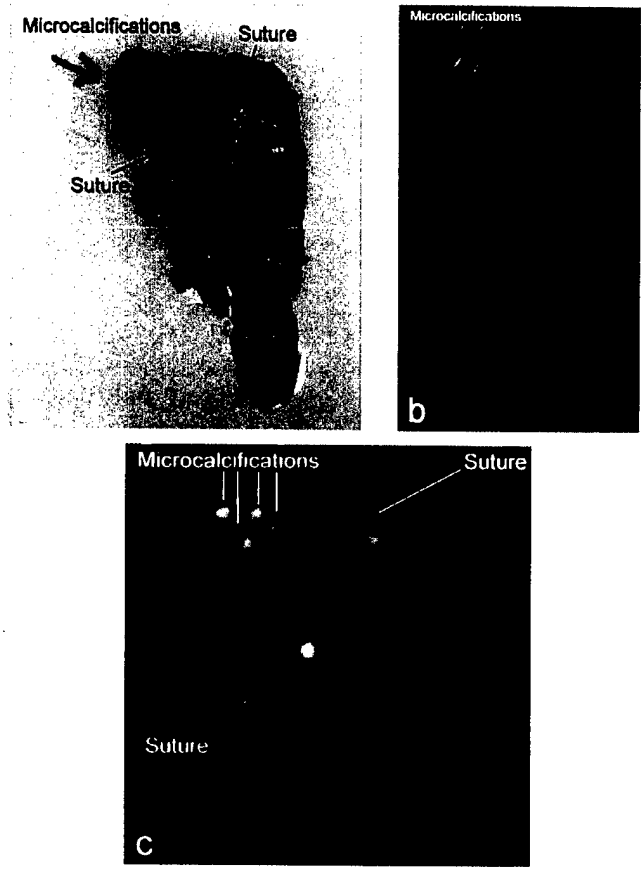

Fig. 3. (a) Photograph of the breast tissue sample. Micro-calcifications are located at the top left corner of the sample (indicated by the arrow). Two sutures are knotted on the tissue as indicators. (b) Tissue x-ray mammogram of the tissue sample. This sample includes four small micro-calcifications at the top left corner. The brightness of the image has been reduced to make the micro-calcifications stand out from the high density tissue at the top left corner of the sample. As a result, most of the tissue is not visible in the x-ray image, except for the calcified region and some bright irregular regions (containing no calcification) at the center. (c) Vibro-acoustic image of the sample in (a) and (b). This image clearly shows four micro-calcifications as bright spots at the top left corner of the tissue sample. The two sutures are also indicated in the image. The location of micro-calcifications shown here matches well with those shown in the x-ray mammogram.

Acknowledgments

This work was supported in part by grant BC971878 from the Army Medical Research and Materiel Command and grant HL 61451 from the National Institutes of Health.

References

1. Fatemi M, Greenleaf JF: Ultrasound-stimulated vibro-acoustic spectrography. Science 1998; 280:82-85.
2. Fatemi M, Greenleaf JF: Vibro-acoustography: An imaging modality based on ultrasound-stimulated acoustic emission. Proc Natl Acad Sci USA (PNAS) 1999; 96:6603-6608.
3. Fatemi M, Greenleaf JF. Probing the dynamics of tissues by the radiation force of ultrasound. Phys Med Biol 2000; 45:1449-1464.
4. Beyer RT: Radiation pressure - the history of a mislabeled tensor. J Acoust Soc Am April 1978; 63(4):1025-1030.
5. Chu B-T, Apfel RE: Acoustic radiation pressure produced by a beam of sound. J Acoust Soc Am 1982; 72(6):1673-1687.
6. Fatemi M, Greenleaf JF: Imaging the viscoelastic properties of tissue: In: M. Fink , J-P Montagner, A. Tourin: Imaging complex Media with Acoustic and Seismic Waves. To be published with the series "Topics in Applied Physics", Springer-Verlag, 1999 (in press).

Appendix B

Contrast Coherent Imaging (CCI) at low mechanical index was used. On a semiquantitative scale the capability, to show macrovascular structures and possible modifications of parenchyma during the basal arterial, portal, and late phases using color or power Doppler with and without echocontrast administration, was evaluated. *RESULTS AND CONCLUSIONS:* Color/power Doppler is widely used for the study of focal liver lesions. Its limitations in terms of sensitivity prevents the possibility of showing the microcirculation. This study demostrates that low MI-CCI and contrast enhancement allow the visualization of both macrovascular and parenchymal circulation characteristics.

Breast Masses

Moderators: Brian S. Garra, MD, and Cynthia L. Rapp, BS, RDMS

3205 Comparison of the Sensitivity of Ultrasound for Demonstration of Benign Versus Malignant Disease at the Time of Needle Localization

Copit DS,* Stassi J, Wang J, Cavanaugh BC *Albert Einstein Medical Center, Philadelphia, PA*

OBJECTIVE: To compare the efficacy of ultrasound (US) in demonstrating benign disease and invasive breast carcinoma after a mammographic abnormality is identified using needle localization and surgical biopsy for confirmation. *METHODS:* During an 18-month period, 220 localizatons for a mammographic abnormality other than calcifications were attempted using US guidance. After placement of the needle with US, position was confirmed mammographically. Cases were considered positive if (1) the needle passed through the mammographic abnormality, and (2) the mammographic lesion was demonstrated in the specimen radiograph. Retrospective review of these cases was performed to determine the number of benign vs. malignant lesions. *RESULTS:* Eighty-four invasive cancers were identified pathologically, of which 73 had a positive US, giving a sensitivity for US of 94.8%. Of the 143 benign cases, 101 had a positive US, giving a sensitivity of 70.6% for benign disease. *CONCLUSIONS:* Although the US characteristics of both benign and malignant disease have been studied, there is little written about the sensitivity of US once a mammographic abnormality is discovered. We have shown that the sensitivity of US for demonstrating confirmed invasive cancer is higher than that for benign disease. Our findings suggest that the overall sensitivity of US for demonstrating invasive cancer once focused on a mammographic finding may be excellent. This has importance in clinical practice in terms of the potential for increasing the positive predictive value of mammography once abnormalities are seen. Further investigation to support these findings will be necessary.

3210 Breast Sonography Complementary to Mammography in the Identification of Malignancy Causing Mammographic Architectural Distortion

Hashimoto BE,* Kramer DJ, Picozzi VJ, Lee ME, Morgan G, Sonntag JS, Boswell S *Virginia Mason Medical Center, Seattle, WA*

OBJECTIVE: To correlate mammographic architectural distortion with breast sonography, pathology, and clinical followup. *METHODS:* We retrospectively reviewed reports from 51,962 mammograms from 2 consecutive years. Additional mammographic views were recommended in 3162/51,962 reports (6%). One hundred eighty-eight of 3162 (6%) of these additional views were performed because of mammographic architectural distortion. In 41/188 (21%), the architectural distortion was associated with another mammographic abnormality (density, mass, or calcification). In 156/197 (79%), architectural distortion was the sole abnormality. In 45/188 cases (24%), breast sonograms were performed in addition to mammograms. Histologic information was available for 50/188 cases (27%). *RESULTS:* Twenty-three of 50 biopsies (46%) performed for mammographic architectural distortion were malignant. This malignant biopsy rate is higher than the overall malignancy rate of all breast biopsies performed on this population during the same time period (30%). Pathology results, radiographic, and clinical followup of 188 lesions demonstrated that mammographic additional views had a sensitivity 70%, specificity 91%, PPV 50%, NPV 96%. For the 45 lesions which were evaluated by both mammography and sonography, sonography demonstrated better sensitivity (sensivity 91%, specificity 64%, PPV 62%, NPV 97%) compared to mammography (sensitivity 82%, specificity 43%, PPV 38%, NPV 90%). If both modalities are combined, the sensitivity improves (sensitivity 100%, specificity 44%, PPV 37%, NPV 100%). *CONCLUSIONS:* Breast sonography may have better sensitivity in identifying malignancy compared to mammography alone. The improvement in sensitivity when both modalities are combined suggests that these tests provide complementary information, which may improve detection of malignancy in this group of patients.

3212 Imaging Breast Microcalcification by Vibro-Acoustography

Fatemi M,* Wold LE, Morton MJ, Greenleaf JF *Mayo Clinic/Foundation, Rochester, MN*

OBJECTIVE: Imaging breast microcalcification in excised tissue by vibro-acoustography. *METHOD:* Vibro-acoustography [Science 280:82-5, 1998] is a novel method evaluating tissue mechanical response at low kHz frequencies. This method utilizes the radiation force of ultrasound to induce low-frequency elastic waves in tissue and detects its response. These waves are detected by an audio hydrophone and can be used to construct an image of the object mechanical properties. Microcalcifications that are much stiffer than the surrounding soft tissue produce a stronger response than the tissue, resulting in high contrast appearance in the final image. Excised breast tissues were scanned by a vibro-acoustography system with a 3-MHz transducer. The vibration frequency of the imaging system was typically in the range of 5 to 28 kHz. High-resolution x-ray tissue mammography of the samples was also obtained and used as control images. *RESULTS:* Vibro-acoustic images of tissue samples provided clear and well defined display of microcalcifications. The number and position of the

microcalcifications matched with those seen in mammography. Microcalcifications as small as 100 microns in diameter could be detected by vibro-acoustography. The presence of microcalcifications was validated by histological study of the samples. *CONCLUSIONS:* Vibro-acoustography can be used for imaging small breast microcalcifications. The non-invasive nature of vibro-acoustography promises in vivo applications, especially in cases where mammography cannot be used either because of high breast density or hazards of x-ray to the patient.

3219 Classification of Breast Lesions Using Multifeature Analysis Procedures

Alam SK,*[1] Lizzi FL,[1] Feleppa EJ,[1] Liu T,[2] and Kalisz A,[1] *[1]Riverside Research Institute, New York, NY, and [2]Department of Radiation Oncology, Columbia University, New York, NY*

OBJECTIVE: Various features in ultrasound gray scale images are used clinically to discriminate benign from malignant breast lesions. These include acoustic features ("echogenicity," "heterogeneity," "shadowing") and morphometric features ("area," "location," "aspect ratio," "border irregularity," "margin definition"). Accordingly, our goal is to develop a family of quantitative descriptors of breast-lesion features to reliably distinguish benign from malignant lesions and thereby reduce the number of unnecessary breast biopsies. These quantitative descriptors are independent of instrument properties and physician expertise, and are applicable to small tumors. *METHODS:* We quantify acoustic features using calibrated spectrum analysis of radio-frequency (RF) echo signals (rather than gray scale images) and we quantify morphometric features using geometric and fractal parameters. RF echo data were acquired during routine ultrasonic examinations prior to biopsy. Gray scale images were generated from RF data, and lesion boundaries and adjacent areas on the images were manually traced. Spectral parameter maps were computed within these areas to derive quantitative measures of acoustic features. Morphometric features were computed by geometric and fractal analysis of manually traced lesion boundaries. *RESULTS AND CONCLUSIONS:* Early results on biopsy-proven cases are promising and show that multifeature analysis may improve discrimination of cancerous and non-cancerous lesions. We have processed data for 119 patients using 8 quantitative features, and produced an ROC-curve area of 0.8727 ± 0.0416. Lesion echogenicity, aspect ratio, a convexity parameter (descriptor of spiculation), and a fractal-dimension measure (descriptor of border irregularity) were the most useful descriptors. Some morphometric features (e.g., the fractal-dimension measure) were particularly effective in lesion classification.

3202 Lactating Adenoma of the Breast: Sonographic Findings

Sonntag JS,* Hashimoto BE *Virginia Mason Medical Center, Seattle, WA*

DESCRIPTION OF CASES: Case 1 is a 35-year-old woman with a right breast mass. The patient is 9 months postpartum and breast feeding. An ultrasound of the palpable abnormality corresponds to a 19 mm circumscribed, ellipsoid mass of mixed echogenicity in the inner right breast at 7 o'clock with bilateral edge shadowing. Case 2 is a 33-year-old pregnant woman with a palpable mass in the outer left breast at 3 o'clock. Ultrasound demonstrates a 51 mm hypoechoic, ellipsoid mass with well circumscribed margins and equal transmission. Case 3 is a 21-year-old pregnant woman with an enlarging, palpable abnormality in the outer left breast at 2 o'clock which has been present for several months. Sonographic evaluation discovers a 12 mm lobulated shadowing mass of mixed echogenicity with circumscribed margins. Case 4 is a 31-year-old woman who is 2 months postpartum with a palpable lump in the outer right breast at 3 o'clock. Ultrasound reveals a 30-mm gently lobulated, ellipsoid mass of mixed echogenicity with equal transmission. *PROOF OF DIAGNOSIS:* All cases were histologically proven lactating adenomas biopsied between 1998 and 2000. *RELEVANCE:* Although rare, lactating adenomas are important sonographic findings. Lactating adenomas typically present as palpable masses in pregnant or lactating women, so sonography is generally the first test performed to evaluate these lesions. The above cases demonstrate the spectrum of sonographic findings of lactating adenomas.

3203 Detection of Silicone Adenopathy in Silicone Gel Breast Implant Patients

McNamara MP Jr,* Punjabi R *MetroHealth Medical Center, Cleveland, OH*

DESCRIPTION OF CASES: Over the last 9 years, we have examined nearly 2000 breast implant patients with ultrasound. Early in our experience, we encountered an implant patient who complained of focal supraclavicular pain and requested that the area be scanned at the completion of her breast implant ultrasound examination. At the site of her concern, a small round hyperechoic mass with a "dirty" acoustical shadow was noted. Given the similarity in appearance to silicone granuloma, a supraclavicular node containing silicone was suspected. The mass was needle localized under ultrasound guidance and pathologically proven as silicone lympadenopathy. Subsequently, we began a systematic search of the remainder of the lymph node chains that drain the breast. As a result, in addition to patients with silicone in intramammary and low axillary (Level 1) nodes, we have subsequently identified patients with silicone-containing nodes in retropectoral (Level 2 and 3), Rotter, supraclavicular, and internal mammary chain lymph nodes in patients with intact and ruptured implants. *PROOF OF DIAGNOSIS:* Diagnosis at each anatomic site was proven with pre-operative localization, operative excision, specimen ultrasound, and histology. *RELEVANCE:* Intramammary and low axillary silicone lymphadenopathy has been reported in the peer reviewed literature. Additionally, one case of internal mammary chain involvement identified with CT has been reported. This paper documents that silicone adenopathy can also affect the other lymphatic chains draining the breast. Further, we illustrate the typical sonographic appearance and the techniques employed to demonstrate it. Most patients with silicone adenopathy had polyurethane-coated implants.

IEEE Transactions on Medical Imaging (submitted April 26, 2001)

Appendix C

Vibro-acoustic Tissue Mammography

Mostafa Fatemi,* Lester E. Wold, Azra Alizad, and James F. Greenleaf, Fellow, IEEE

M. Fatemi, A. Alizad, and J. F. Greenleaf are with the Basic Ultrasound Research Laboratory, Department of Physiology and Biophysics, Mayo Clinic and Mayo Foundation, Rochester, MN 55905; L. E. Wold is with the Laboratory of Medicine and Biology, Mayo Clinic and Mayo Foundation

This research was supported by grant DAMD17-98-1-8121 from the Army Medical Research and Materiel Command.

Abstract—A novel method for detection and imaging of microcalcifications in breast tissue is presented. The method, called vibro-acoustography, uses the radiation force of ultrasound to vibrate the tissue at low (kHz) frequency and records the resulting response to produce images that are related to the hardness of the tissue. The method is tested on human breast. The resulting vibro-acoustographic images are in agreement with the corresponding x-ray mammography images of the specimens. The existence of microcalcifications in locations indicated by vibro-acoustography is confirmed by histology. Microcalcifications as small as 110 microns in diameter are detected by this method. Tissue density and inhomgeneties do not seem to interfere with detection of microcalcifications.

Index Terms—Vibro-acoustography, Microcalcifications, Breast, Mammography, Ultrasound

I. INTRODUCTION

X-ray mammography is the only imaging modality clinically used currently for detection of breast microcalcifications. The widespread use of screening mammography has resulted in the increased detection of microcalcifications. The spectrum of breast lesions associated with microcalcifications ranges from benign fibrocystic changes to atypical ductal hyperplasia to ductal carcinoma in-situ. The mammographic detection of microcalcifications frequently results in additional diagnostic studies, including: spot magnification mammographic views, stereotaxic biopsy, and wire-localized needle biopsies. Follow-up of microcalcifications that are not biopsied, or that are benign by stereotaxic biopsy, may require additional mammograms, e.g., at six-month intervals. This results in significant additional costs, discomfort, anxiety, and some increase in x-ray exposure [1]. Recent changes in American Cancer Society (ACS) and National Cancer Institute (NCI) screening guidelines for women in their forties will increase both the number of mammograms and the number of detected microcalcifications, with resultant increased costs and morbidity. American Cancer Society (ACS) recommends that a baseline mammogram be obtained at 35. Between ages 40 and 50, the ACS recommends that mammography should be obtained every 2 years, and that annual surveillance take place after age 50. In women at "high" risk for breast cancer, it is possible to increase this surveillance. The initial baseline mammogram can be moved up earlier than age 35, although it is well known that mammography is less sensitive in younger women. Furthermore, annual mammography can begin at age 40 rather than age 50 [2].

There exist subsets of women for whom mammographic screening and follow-up is limited by reduced mammographic sensitivity. The ACS estimates that about half of all women in America have fibrocystic breasts and many of them have very dense breast tissue. For this group, failure to detect cancer on their mammogram may be as high as 15-25% [3], [4]. Mammography is more

effective in detecting occult malignancy as age increases and the breast becomes more fatty. It is the density of the breast on film screen mammography that most directly affects the risk for false-negative and false-positive interpretation [5], [6]. Several factors impact breast density. Age is the most significant factor, with more pre-menopausal women, especially in the 40- to 49-year age group, having breasts that are more glandular and thus more dense. For pre-menopausal - women mammographic sensitivity may be increased by scheduling evaluation the first two weeks of their cycle corresponding with the follicular phase [7], [8]. Pregnant or lactating women may have extremely dense breast tissue, which may affect the sensitivity of mammography; also these conditions are a relative contraindication for x-ray mammography, and thus limit its usefulness. Some studies have shown hormone replacement therapy, commonly used in postmenopausal patients, reduces the sensitivity of mammographic screening [9], [10], [11]. The sensitivity or accuracy of film screen mammography is also influenced by the experience of the radiologist. The most experienced radiologist had the highest sensitivity in diagnosing breast cancer [12]. Finally, the ionizing nature of the x-ray mammography limits its frequent use.

To overcome some of these variables that impact the predictive value of mammography, a number of new technologies are currently being explored. Investigators have utilized alternative breast imaging methods, such as MRI and conventional ultrasound for imaging breast microcalcifications. Scintimammography and contrast-enhanced MRI are not sufficiently sensitive to detect clinically significant microcalcifications [13]. Similarly, conventional medical ultrasound imaging is not currently considered a sufficiently reliable to visualize breast microcalcifications [14], [15], [16]. Microcalcification visualization by ultrasound is limited by a number of factors specific to this technique, such as speckle noise [16]. Although ultrasound can be used as an effective adjunct to mammography in detecting breast cancer [17], this technique will miss occult

cancers where microcalcification is the only clue to malignancy. Thus, a sensitivity of only 63% was found in a study by Kasumi [18]. However, Yang, et al. [19] reported that using high-resolution ultrasound and x-ray mammography as the gold standard resulted in a sensitivity of 95% and specificity of 87% and accuracy of 91% in the detection of microcalcifications when these calcifications are within a mass lesion [19]. It should be noted that the presence of a mass lesion and its appearance in the ultrasound image could have been instrumental in the localization and identification of microcalcifications in such studies.

Microcalcifications are mainly composed of hydroxyaptite [16], [20], which is a very hard material compared to beast soft tissues. Therefore, an imaging modality that is sensitive to the elastic properties of tissues would be suitable for detection of microcalcifications. This group of imaging techniques is called elasticity imaging.

The general approach in elasticity imaging is to measure the response of tissue to an excitation force. An interesting strategy for producing the necessary excitation is to use the radiation force of ultrasound. This approach allows one to generate the force directly inside an organ. Several researchers have previously investigated the use of ultrasound radiation pressure for tissue characterization purposes. Sugimoto et al. [21] presented a method to measure tissue hardness by using the radiation force of a single ultrasound beam. In this method, the impulsive radiation force was used to generate localized deformation of tissue. Resulting transient deformation was measured as a function of time by ultrasound Doppler method. Nightingale et. al. [22] have studied the radiation force of ultrasound in a method named "remote palpation" to evaluate lesions in breast. They also used ultrasound pulse-echo technique to detect tissue displacement. None of the above methods have sufficient spatial resolution for detection of breast microcalcifications. Walker [23] evaluated the deformation of soft tissues including breast by the

radiation force of ultrasound. It should be noted that motion detection by ultrasound techniques (at diagnostic frequencies) becomes technically difficult if the motion is less than 1 micron. Walker predicted that the displacement produced by absorption of an ultrasound beam of moderate intensity (1 W/cm^2) in breast tissue is too small (less than 0.01 microns) for ultrasound detection.

Vibro-acoustography is a new imaging method based on the radiation force of ultrasound [24], [25]. This method is particularly useful in detecting hard inclusions in soft material. For example, vibro-acoustography has been used to image calcifications in human arteries [26], [27], [28]. A comparative study of vibro-acoustography with other radiation force methods for tissue elasticity imaging is presented in [27]. Unlike other radiation force methods, the spatial resolution of vibro-acoustography is in the sub-millimeter range, which makes the technique suitable for imaging microcalcifications [29], [30].

Here, we present an application of vibro-acoustography for detection of breast microcalcifications. We may call the new method vibro-acoustic tissue mammography. We shall image human breast tissue specimens with vibro-acoustography and compare the results with those of high-resolution x-ray tissue mammography and validate the presence of calcifications in the tissue by histology.

II. METHODS AND MATERIALS

A. Theory of Radiation Force

Radiation force is generated by a change in the energy density of an incident acoustic field. Consider a collimated ultrasound beam interacting with an object. The radiation force arising from this interaction has a component, F, in the beam direction. This component is proportional to the time average energy density of the incident wave $\langle E \rangle$ and the projected area of the object, S, as:

$$F = d_r S < E >, \qquad (1)$$

where d_r is the drag coefficient, and is a function of the scattered and absorbed power by the object. For the simple case of a reflecting plane target, d_r is proportional to the power reflection coefficient. In vibro-acoustography [17], this force is used for imaging. This is accomplished by probing the object point-by-point. This technique ideally requires the stress field to be confined to a point, while its amplitude oscillates at selected frequencies.

To generate a localized oscillatory stress field, two intersecting CW focused ultrasound beams of different frequencies are used. It is only in the intersection region that the ultrasound field energy density is sinusoidally modulated, and hence, the field can generate an oscillatory radiation force by interacting with the object.

The ultrasound beams can be shaped in a variety of ways for this purpose. An interesting configuration that results in a radially symmetric modulated field is obtained when two coaxial, confocal transducer elements are used (Fig. 1). In this case, we consider a two-element spherically focused annular array, consisting of a central disc with the radius of a_1, and an outer ring with the inner radius of a_2' and the outer radius of a_2. The common focal length of the elements is z_0. We also assume that the elements are excited by two CW signals at frequencies ω_1 and $\omega_2 = \omega_1 + \Delta\omega$. Let us assume that the beams are propagating in the z direction with the joint focal point at $z=0$. The resultant field on the $z=0$ plane may be written as:

$$p(t) = P_1(r)\cos[\omega_1 t + \psi_1(r)] + P_2(r)\cos[\omega_2 t + \psi_2(r)], \qquad (2)$$

where $P_1(r)$ and $P_2(r)$ are the pressure radial profiles in r direction with $\psi_1(r)$ and $\psi_2(r)$ being the associated phase functions across the focal plane. For the transducer described above, these amplitude functions can be written as [31]:

$$P_1(r) = \rho c U_{01} \frac{\pi a_1^2}{\lambda_1 z_0} \text{jinc}\left(\frac{r a_1}{\lambda_1 z_0}\right), \qquad (3)$$

and

$$P_2(r) = \rho c U_{02} \frac{\pi}{\lambda_2 z_0}\left[a_2^2 \text{ jinc}\left(\frac{r a_1}{\lambda_1 z_0}\right) - a_2'^2 \text{ jinc}\left(\frac{r a_2'}{\lambda_2 z_0}\right)\right], \qquad (4)$$

where $\lambda_i = 2\pi/\omega_i$ for *i=1, 2*, are ultrasound wavelengths at the *i-th* transducer element, and U_{0i}, *i=1, 2*, is the velocity amplitude at the corresponding element. Also, $\text{jinc}(X) = J_1(X)/\pi X$, where $J_1(X)$ is the first order Bessel function of the first kind. For well-focused beams, $P_1(r)$ and $P_2(r)$ diminish quickly away from the origin.

It can be shown that the short time average of the acoustic energy density in the intersection region has slow variations at frequency $\Delta\omega$ about its long time average (mean). Denoting this low frequency component by $e_{\Delta\omega}(t)$, we can write:

$$e_{\Delta\omega}(t) = \frac{P_1(r_0)P_2(r_0)}{\rho c^2}\cos[\Delta\omega t + \Delta\psi(r_0)], \qquad (5)$$

where ρ is the density, *c* is the sound speed, and $\Delta\psi = \psi_2(r) - \psi_1(r)$. Now, consider a planar target on the focal plane. Referring to Eq. (1) and considering that the average energy density is position and time dependent in this case, the normal component of the time varying force on an area element *dS at* $r = r_0$ with a local drag coefficient $d_r(r_0)$ is:

$$f_{\Delta\omega}(r_0, t) = \frac{P_1(r_0)P_2(r_0)}{\rho c^2}\cos[\Delta\omega t + \Delta\psi(r_0)] d_r(r_0) dS\,. \qquad (6)$$

This function also represents the distribution of force, or the stress field, on the focal plane. The total force on the object can be found by integrating the above incremental force over the projection area *S* on the focal plane.

$$\tilde{f}_{\Delta\omega}(r_0,t)=\left|\overline{F}_{\Delta\omega}\right|\cos(\Delta\omega t+\Delta\overline{\psi}), \qquad (7)$$

where $\overline{F}_{\Delta\omega}$ is the complex amplitude of the total force and $\Delta\overline{\psi}$ is the associated phase. For a well-focused beam S is very small, and hence, the force can be thought of as an oscillating point-like force applied to the object at the origin.

B. Vibro-acoustography system

To explain the imaging method, we consider an oscillating point force, $\overline{F}_{\Delta\omega}$, applied to a point in the object. This force vibrates the object. Object vibrations result in the emission of an acoustic field in the surround energy that can be detected by a microphone (or hydrophone in water). The system diagram is shown in Fig. (1). The complex amplitude of acoustic emission pressure field, $P_{\Delta\omega}$, can be written as [17]:

$$P_{\Delta\omega}=\rho c^2 H_{\Delta\omega}(l)Q_{\Delta\omega}\overline{F}_{\Delta\omega}, \qquad (8)$$

where $Q_{\Delta\omega}$ is a complex function representing the mechanical frequency response of the object at this point, and $H_{\Delta\omega}(l)$ represents the combined frequency response of the propagation medium and the microphone located at distance l from the object. It is assumed that $H_{\Delta\omega}(l)$ to be unchanged for any target point in the object. Now, by scanning the object at a fixed frequency $\Delta\omega$ and recording the acoustic emission signal, one can obtain the spatial distribution of $Q_{\Delta\omega}F_{\Delta\omega}$ (within a constant multiplier) which can be mapped into an image, displaying object morphology.

The point-spread-function (PSF) of this system is defined as the image of a point target located on the focal plane [17]. This function is proportional to the radiation stress field on the focal plane. This function can be found in an analytical form by combining Eqs. (3), (4) and (6). The amplitude of this function can be written as [17]:

$$h(r)=\frac{1}{a_2^2-a_2'^2}\,\mathrm{jinc}\left(\frac{ra_1}{\lambda_1 z_0}\right)\left[a_2^2\,\mathrm{jinc}\left(\frac{ra_2}{\lambda_2 z_0}\right)-a_2'^2\,\mathrm{jinc}\left(\frac{ra_2'}{\lambda_2 z_0}\right)\right]\exp(j\Delta\overline{\psi}) \qquad (9)$$

Assuming a 3-MHz-transducer with the outer diameter of 45 mm, inner disk diameter of 29.6 mm and a gap of 2 mm between the inner disk and the outer ring, and a focal length of 70 mm, the amplitude of the resulting PSF function for $\Delta f = \Delta\omega/2\pi = 7.3$ kHz is shown in Fig. (2). The spatial resolution of the system, defined by the diameter of the central lobe, is about 0.7 mm.

C. Experimental Setup

The experimental setup is shown in Fig. (1). The experiments were conducted in a water tank. (In a system designed for in vivo imaging the transducers can be placed in contact with the soft tissue instead of using water.) A two-element confocal ultrasound transducer array was positioned such that the beams meet the object at their joint focal point. Transducer specifications are as those in the previous section. The elements are driven by two stable RF synthesizers (HP 33120A) at frequencies of 3MHz and 3MHz+Δf. Sound produced by the object vibration was detected by a submerged hydrophone (ITC model 680) placed within the water tank. The received signal is filtered and amplified by a programmable filter (Stanford Research Systems, SR650) to reject the noise, then digitized by a 12-bits/sample digitizer (National Instruments VXI-1000) at the rate sufficiently higher than the Nyquist rate for the particular used. Data are recorded on a computer disc.

D. Experiment Procedure

In order to evaluate the capability of the system in imaging small particles about the size of a common breast microcalcification, we constructed a test object comprising of four small glass beads, ranging from 260 to 400 microns in diameter imbedded in a block of tissue mimicking gel.

The resulting vibro-acoustography image is shown in Fig. (3), demonstrating the capability of the system in detecting and imaging beads that are at least 260 microns in diameter.

Tissue experiments were conducted on excised human breast tissue samples. Patients' records were reviewed to identify tissues with high probability of having microcalcifications. Selected tissues were cut into (approximately) 3x3 cm pieces and imaged using a high-resolution x-ray mammography machine. The x-ray mammograms were then read to identify presence of microcalcifications. Tissue pieces identified with microcalcification were each mounted by a few droplets of glue on a latex sheet and secured in a scanning bracket. This bracket is designed to hold the tissue piece in the water for acoustic scanning. Glue drops were carefully placed on areas away from the region with microcalcifications. Small pieces of suture were sewed to the tissue and used as identification marks. For this purpose, small knots are placed at different positions on the tissue away from microcalcifications. These markers could be seen in vibro-acoustography, x-ray (often very dim), and photography images.

Specimen x-ray mammographic images were obtained from each mounted sample. Each x-ray image was used as a reference for comparison with the corresponding vibro-acoustography image. The system illustrated in Fig. (1) was used to obtain Vibro-acoustography images of tissue samples. Sections of the tissue identified with microcalcification were then cut for histologic study to identify microcalcifications and validate the imaging results.

III. RESULTS

Figure (4-a) shows the photograph of a breast specimen mounted on the scanning bracket. Sutures are knotted on the tissue for identification purpose. Figure (4-b) shows the x-ray mammogram of the selected tissue pieces mounted on the scanning bracket. The sutures are barely

visible. Microcalcifications can be seen on the top left of this x-ray in a high-density sclerotic region. This sample was then scanned in the water tank. The vibro-acoustography image of the tissue, at $\Delta f = 25$ kHz, is shown in Fig. (4-c). Microcalcifications can be seen in this image as bright spots. Note that the number of microcalcifications matches with the corresponding spots in the x-ray mammography. Also noticeable is that tissue inhomogeneities appear dim and do not interfere with calcification in vibro-acoustic image. Microcalcifications identified by vibro-acoustography were verified histologically. Figure (4-d) shows the histology of the region around the calcifications. The breast parenchyma shows atypical lobular hyperplasia and microcalcifications in the lobules. We measured the size of the microcalcification at the lower left, by measuring the spot size in the x-ray mammogram, and found out it is approximately 110 microns in diameter.

Figure (5-a) shows the photograph of second breast tissue specimen mounted on the scanning bracket. Figure (5-b) is the x-ray mammogram of this tissue and shows the microcalcifications at the center of the image. Figure (5-c) shows the vibro-acoustic image of this tissue at 22 kHz. Microcalcifications can be seen as bright spots at same location as in the x-ray. The breast parenchyma histologically showed comedo type ductal carcinoma in situ, with calcifications in regions of comedo necrosis.

Figure (6-a) shows the x-ray of mammogram of another breast tissue specimen with a large microcalcification. Figure (6-b) shows the corresponding vibro-acoustic image, with the microcalcification shown as a bright spot and the background soft tissue relatively dim.

IV. DISCUSSION

Experimental vibro-acoustography images presented in this report demonstrate two important facts: (1) The vibro-acoustography imaging method is capable of detecting small microcalcifications in breast tissue; (2) Microcalcifications can be delineated from other tissue inhomogeneities. Results shown here also indicate that such images have high spatial resolution (700 microns), the capability of detecting small (about 110 micron in diameter and above) microcalcifications, no speckles, good contrast, and high signal to noise ratio.

A comparison between the vibro-acoustography image Fig. (4-b) and the corresponding x-ray mammography Fig. (4-c) reveals an interesting capability of vibro-acoustography method. High-density sclerotic tissue in the region surrounding the microcalcification absorbs a great deal of x-ray energy; hence, the x-ray image shows very low contrast within this region and as a result microcalcifications are barely visible. However the vibro-acoustography image delineates these calcifications with high contrast. This demonstrates that some tissues that are radiologically opaque may be transparent in vibro-acoustography images giving the potential to detect calcification in radiologically dense breasts.

The halo seen around the images of each microcalcification is an artifact of the vibro-acoustography system. This effect is seen more clearly in the PSF image shown in Fig. (2). Multiple rings around the center spot are due to the sidelobes of the Bessel functions that appear in the PSF function (Eq. (9)) as discussed in the previous section.

Another artifact is due to the glue used to bond the tissue specimens to the latex sheet. We used small droplets of instant glue (Krazy Glue brand) for this purpose. This type of glue produces a relatively strong acoustic emission making it visible in vibro-acoustography images. Figure (7) shows a vibro-acoustography image of three droplets of this glue on a latex sheet, resembling

images of breast microcalcification. To avoid mistaking glue droplets for microcalcifications, we marked the glued region of tissue and took extra precautions to locate these regions on the vibro-acoustography images.

The choice of vibration frequency Δf used in each experiment was, to some extent, determined by the resonance frequencies of the water tank. The acoustic emission field resulting from vibrations of microcalcifications is very small. To facilitate the detection process, we often chose the vibration frequency to correspond to one of the resonance frequencies of the water tank. This way, the water tank acts as an amplifier to improve the signal-to-noise ratio.

In the present study, we imaged tissue samples only in two dimensions (i.e., a single slice). However, the ultrasound beam used here produces a stress field that is confined in three dimensions. Therefore, it is possible, in principle, to selectively scan several slices of the object at different depths to produce a three-dimensional (volume) image of the object.

Vibro-acoustic detection and follow-up of microcalcifications has many clinical potentials. These include, but are not limited to:

- Detection of microcalcifications in the breast of women who are younger and/or have radiologically very dense breast. It is important to know that ultrasound can easily penetrate a radiologically dense tissue.
- Detection of microcalcification in pregnant or lactating women.
- Detection of microcalcification in women who are at very high risk of breast cancer, i.e., known or suspected carriers of BRCA1 or BRCA2 genes.
- Supplemental information to standard mammographically detected microcalcifications (analogous to the supplemental use of ultrasound in the diagnostic evaluation of breast masses).

- Follow-up study at six-month intervals for women with microcalcification between their annual mammograms, obviating the need for additional x-ray exposure.
- Follow-up of known microcalcification in women who are pregnant or lactating at the time they would be due for mammogram follow-up.
- Women with ataxia-telangiectaisa have an increased risk of many cancers, including breast cancer. Homozygotes are 0.2-0.7% of the United States' population. Even heterozygotes, who comprise 7% of the general population, have a five-fold increased risk of breast cancer. Screening mammography, a source of ionizing radiation, could contribute to the increased breast cancer cases seen in this population.
- Detection of microcalcifications in women with radio-opaque breast implants.

V. SUMMARY

In this paper, we presented a noninvasive imaging method for detecting microcalcifications in breast tissue. This method uses ultrasound in a fundamentally new way to image the tissue at low (kHz range) frequencies, producing high signal-to-noise, and speckle free images.

The spatial resolution of such images is determined by the focal beamwidth of the two-element transducer, which was in the order of 0.7 mm for the transducer used here. Experiments were conducted on human breast tissue specimens. X-ray tissue mammography images were used for initial identification of microcalcifications, and also as reference images for comparison with the corresponding vibro-acoustography images. Tissue histology was also used to validate presence of microcalcification.

Results indicate that microcalcifications associated with a variety of breast pathology, including those located in high-density or sclerotic regions of tissue, can be detected by vibro-

acoustography. Microcalcifications that as small as 110 microns in diameter were detected by vibro-acoustic tissue mammography.

Further development of the vibro-acoustic tissue mammography may lead to a novel imaging tool for in-vivo applications. This method can be considered as a non-ionizing alternative to the conventional x-ray mammography, which may be useful for such cases as pregnant patients, were the use of ionizing radiation is not allowed. Also, it is potentially useful for imaging dense breast where the use of conventional x-ray technique may be limited.

ACKNOWLEDGMENT

The authors are grateful to the following individuals for their valuable work during the course of this study: Dr. Ruth E Johnson for valuable comments on the clinical aspects of microcalcification in breast, Tammy Distad for providing post-surgical tissue specimens, Mary Siewert for providing tissue x-rays, Dr. Marylin Morton for reading x-ray mammograms, Randall Kinnick for laboratory support and scanning tissues, Danielle Cook for scanning some of the tissues, Dr. Kazunori Kanehira for histologic evaluation of tissues, Julie Patterson for graphic support, and Elaine Quarve for secretarial assistance. This research was supported by grant DAMD 17-98-1-8121 from the Army Medical Research and Material Command.

REFERENCES

1. M. D. Abeloff, A. S. Lichter, J. E Niederhuber, L. J. Pierce, and R .R. Love, "Breast," in: M. D. Abeloff: *Clinical Oncology*, chap. 75, pp. 2051-2138, 2nd Ed., Churchill Livingstone, New York, 2000.
2. G. D. Dodd, "American Cancer Society guidelines on screening for breast cancer," Cancer, vol. 69(7), pp.1885-1887, 1992.
3. (Anonymous authors) Screening recommendations of the forum panel. J Gerontol, p 47, Spec No. 5, Nov. 1992
4. Fletcher SW, Black W, Harris R, et al: Report of the International Workshop on Screening for Breast Cancer. J. Natl. Cancer Inst., 85(30):1644-1656, 1993.
5. K. Kerlikowske, "Effect of age, breast density, and family history on the sensitivity of first screen mammography," JAMA, vol. 276(1), pp. 33-37, July 1996
6. C. D. Lehman, E. White, S. Peacock, and M. J. Drucker, "Urban N. Effect of age and breast density on screening mammograms with false-positive findings," Am. J. Roentgenol., vol. 173(6), pp. 1651-1655, Dec. 1999.
7. C. J. Baines, M. Vidmar, G. McKeown-Eyssen, and R. Tibshirani, "Impact of menstrual phase on false-negative mammograms in the Canadian National Breast Screening Study," Cancer, vol. 80(4), pp. 720-724, Aug. 1997.
8. E. White, P. Velentgas, M.T. Mandelson, et al. "Variation in mammographic breast density by time in menstrual cycle among women aged 40 to 49 years," J. Natl. Cancer Inst., vol. 90(12), pp. 906-910, June 1998.

9. M. B. Laya, D. B. Larson, S. H. Taplin, and E. White, "Effect of estrogen replacement therapy on the specificity and sensitivity of screening mammography," J. Natl. Cancer Inst., vol. 88(10), pp. 643-649, 1996.

10. J. C. Litherland, S. Scotland, D. Hole, and C. Cordiner, "The effect of hormone replacement therapy on the sensitivity of screening mammograms," Clin. Radiol., vol. 54(5), pp. 285-288, May 1999.

11. A. M. Kavanagh, H. Mitchel, and G. G. Giles, "Hormone replacement therapy and accuracy of mammographic screening," Lancet, vol. 355(9200), pp. 270-274, Jan. 2000.

12. L. Liberman, A. F. Abramson, F. B. Squires, et al., "The breast imaging reporting and data system-positive predictive value of mammographic features and final assessment categories," Am. J. Roentgenol., vol. 171(1), pp. 35-40, July 1998.

13. R. Tiling R, I. Khalkhali, H. Sommer, R. Link, R. Moser, F. Willemen, T. Pfluger, K. Tats, and K. Hahn, "Limited value of Scintimammography and contrast-enhanced MRI in the evaluation of microcalcification detected by mammography," Nucl. Med. Common, vol. 19(1), pp. 55-62, Jan. 1998.

14. A. J. Potterton, D. J. Peakman, and J. R. Young, "Ultrasound demonstration of small breast cancers detected by mammographic screening," Clin. Radiol., vol. 49, pp. 808-813, Nov. 1994.

15. P. B. Guyer, K. C. Dewbury, D. Warwick D, J. Smallwood, and I. Taylor, "Direct contact B-scan clinical ultrasound in the diagnosis of solid breast masses," Clin. Radiol., vol. 37(5), pp. 451-458, Sept. 1986.

16. M. E. Anderson, M. S. Soo, R. C. Bentley, and G. E. Trahey, "The detection of breast microcalcifications with medical ultrasound," J. Acoust. Soc. Am., vol. 101(1), pp. 29-39, Jan. 1997.

17. H. M. Zonderland, E. G. Cokerkamp, J. Hemans, M. J. van de Vijver, and A. E. Van Voorthuisen, "Diagnosis of breast cancer: contribution of US as an adjunct to mammography," Radiol., vol. 213(2), pp. 413-422, Nov. 1999.

18. F. Kasumi, "Can microcalcifications lacted within breast carcinomas be detected by ultrasound imaging?" Ultrasound Med. Biol., vol. 14(suppl.1), pp. 175-82, 1988.

19. W. T. Yang, M. Suen, A. Ahuja, and C. Metreweli, "In vivo demonstration of microcalcification in breast cancer using high resolution ultrasound," Br. J. Radiol, vol. 70, pp. 685-690, July 1997.

20. D. E. Grenoble, J. L. Katz, Dunn, K. L. Murty, and R. S. Gilmore, "The elastic properties of hard tissues and apatites," J. Biomed. Mater. Res., vol. 6(3), pp. 221-233, May 1972.

21. T. Sugimoto, S. Ueha, and K. Itoh, "Tissue hardness measurement using the radiation force of focused ultrasound," IEEE Ultrason. Symp. Proc., pp. 1377-1380, 1990.

22. K. R. Nightingale, R. W. Nightingale, M. T. Palmeri, and G. E. Trahey, "A finite element model of remote palpation of breast lesions using radiation force: factors affecting tissue displacement," Ultrason. Imag, vol. 22(1), pp. 35-54, Jan. 2000.

23. W. F. Walker, "Internal deformation of a uniform elastic solid by acoustic radiation force," J. Acoust. Soc. Am., vol. 105(4), pp. 2508-2558, April 1999.

24. M. Fatemi, and J. F. Greenleaf, "Ultrasound stimulated vibro-acoustic spectroscopy," Science, vol. 280, pp. 82-85, April 1998.

25. M. Fatemi and J. F. Greenleaf, "Vibro-acoustography. An imaging modality based on ultrasound stimulated acoustic emission," Proc. Nat. Acad. Sci. USA, vol. 96, pp. 6603-6608, June 1999.

26. J. F. Greenleaf, R. L. Ehman, M. Fatemi, and R. Muthupillai, "Imaging elastic properties of tissue," in: F. A. Duck, A. C. Baker, and H. C. Starrit. *Ultrasound in Medicine,* chap.14, Institute of Physics Publishing, Philadelphia, 1998.

27. M. Fatemi and J. F. Greenleaf, "Probing the dynamics of tissue at low frequencies with the radiation force of ultrasound," Phys. Med. Biol., vol. 45, pp.1449-1464, 2000.

28. M. Fatemi and J. F. Greenleaf, "Imaging the viscoelastic properties of tissue," in: M. Fink, J-P. Montagner, and A. Tourin: *Topics in Applied Physics*. Springer, Heidelberg, Berlin 2001, vol. 82 (in press).

29. M. Fatemi and J. F. Greenleaf: "Imaging and evaluating the elastic properties of biological tissues." BMUS Bulletin (The British Medical Ultrasound Society), vol. 8(4), pp.16 and 18, Nov. 2000.

30. M. Fatemi and J. F. Greenleaf, "Vibro-acoustography system modeling," Dept. of Defense Breast Cancer Research Program, Era of Hope Proc., vol. I, p. 192, June 2000.

31. P. M. Morse P M and K. U. Ingard, 1968 *Theoretical Acoustics*, New York: McGraw- Hill.

Legends

Fig. 1. Vibro-acoustography system diagram. The system includes a focused confocal transducer, (details shown on the left) consisting of a center disk and an outer ring. Two continuous-wave generators drive these elements at slightly different frequencies. The transducer is focused on the object, with the beams interacting at the joint focal point to produce an oscillating radiation force on the object at the difference frequency. This force causes the object to vibrate, and as a result an acoustic emission field is produced in the surrounding medium. This field is detected by the hydrophone and filtered by a bandpass filter centered at the difference frequency. The amplitude of the resulting signal, detected by the detector, is used to modulate the intensity of the image at a point corresponding to the position of the beam on the object. The image is formed by raster scanning of the object. The experiments take place in a water tank (not shown) containing the transducer, hydrophone, and the object. The object, such as a tissue specimen, is secured on a latex sheet attached to a bracket for the scanning process.

Fig. 2.Theoretical point spread function of the vibro-acoustography system.

Fig. 3. Image of glass beads in gel. This image is obtained by scanning the gel phantom. This image covers an area of 20 mm by 20 mm, scanned at 0.2 mm/pixel. The beads are located about 10 mm deep inside the gel. The diameter of the top bead is about 260 microns, and the diameter of the largest bead is about 400 microns. The vibration frequency was set at 53.5 kHz.

Fig. 4. Vibro-acoustography of the first specimen. (a) Photograph of a breast specimen mounted on the scanning bracket. (b) The x-ray mammogram of the selected tissue pieces mounted on the scanning bracket. Microcalcifications can be seen on the top left of this x-ray. (c) Vibro-acoustography image of the tissue at 25 kHz. Microcalcifications can be seen in this image as bright spots on the top left. (d) Histology of the tissue specimen around the region with some microcalcifications.

Fig. 5. Vibro-acoustography of the second specimen. (a) Photograph of the tissue specimen mounted on the scanning bracket. (b) X-ray mammogram of (a), showing some microcalcifications at the center of the image. (c) Vibro-acoustography of (a). Microcalcifications can be seen as bright spots at same location as in the x-ray.

Fig. 6. Vibro-acoustography of the third specimen. (a) X-ray mammogram of the tissue sample showing a large microcalcification. (b) Vibro-acoustography image of (a).

Fig. 7. Vibro-acoustography of the instant glue drops. The glue drops (about 1 mm in diameter) are placed on a latex sheet.

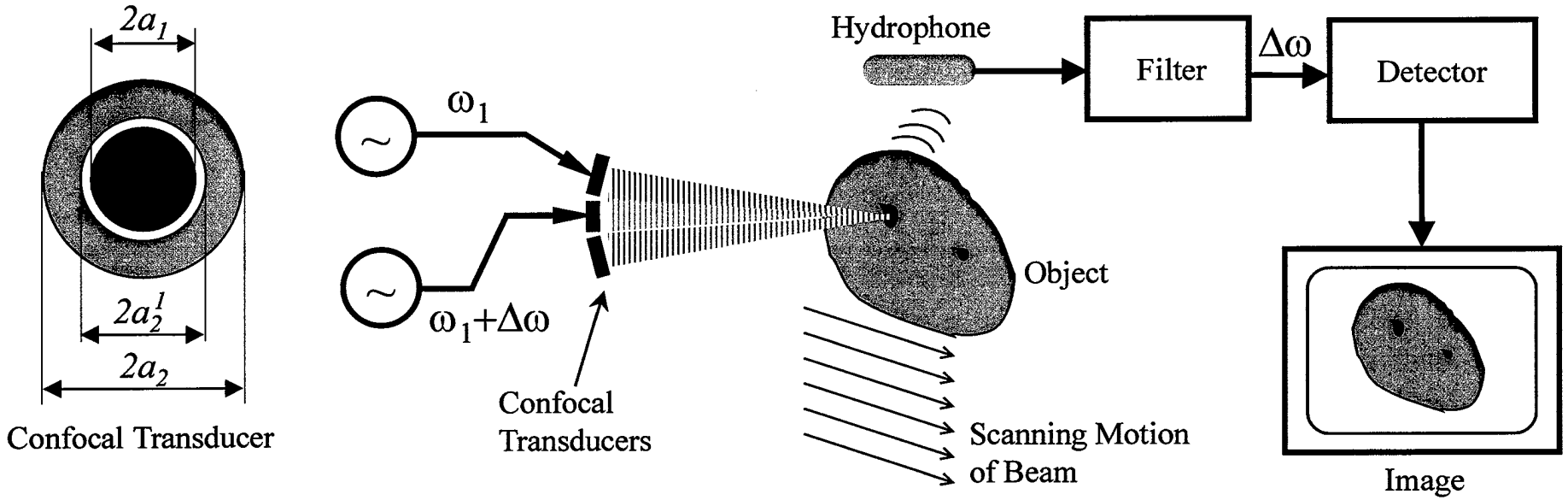

Fig. 1

Figure 1

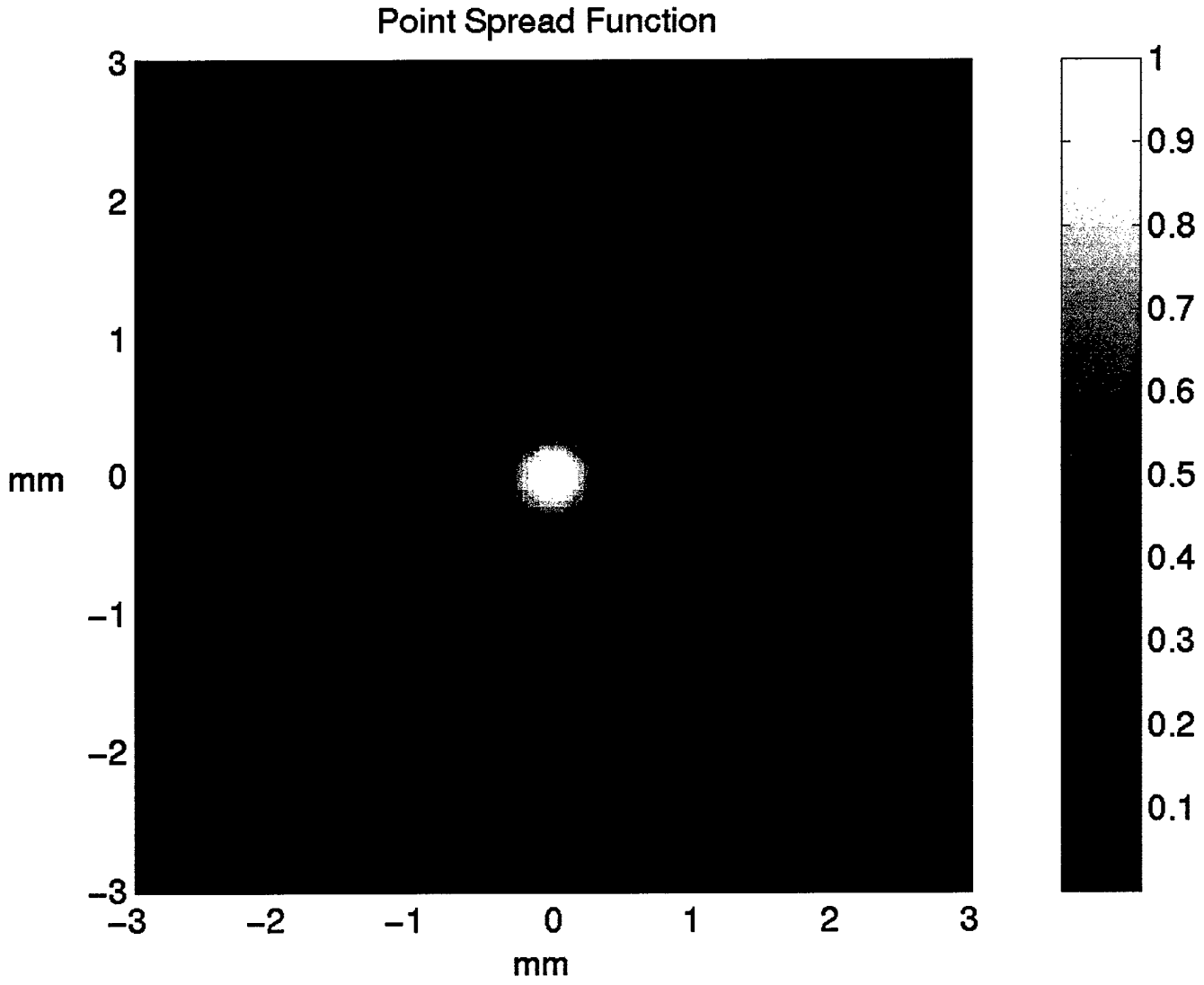

Fig. 2

Figure 2

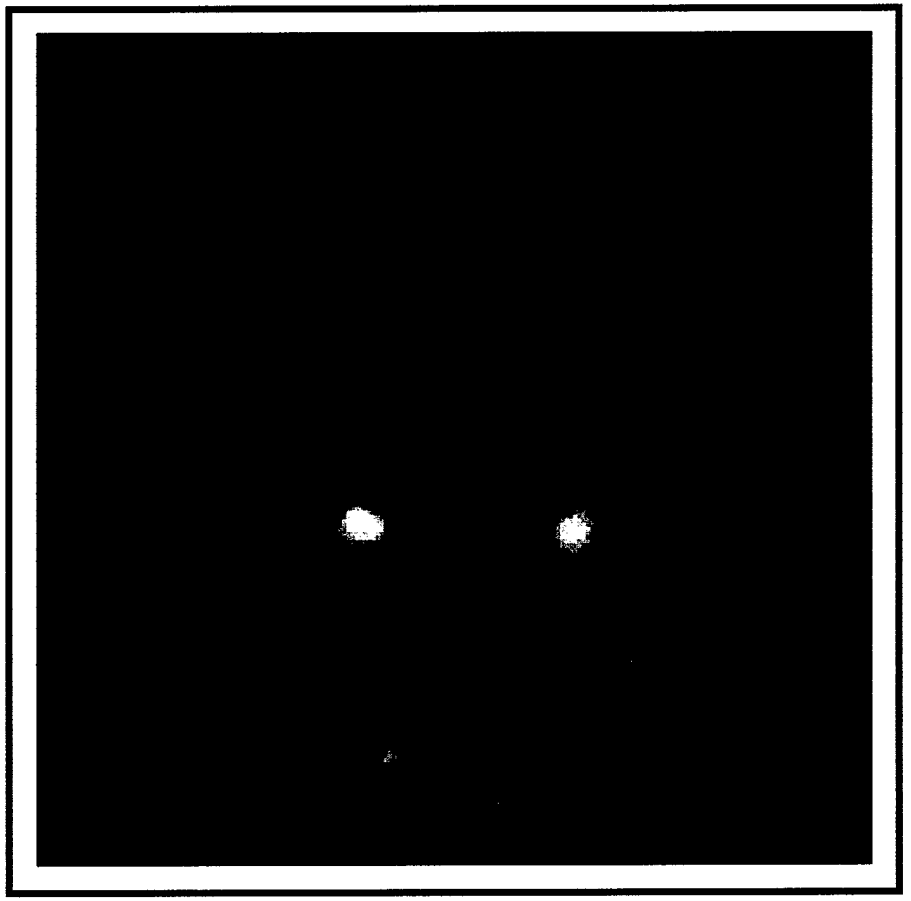

Figure 3

Fig. 3

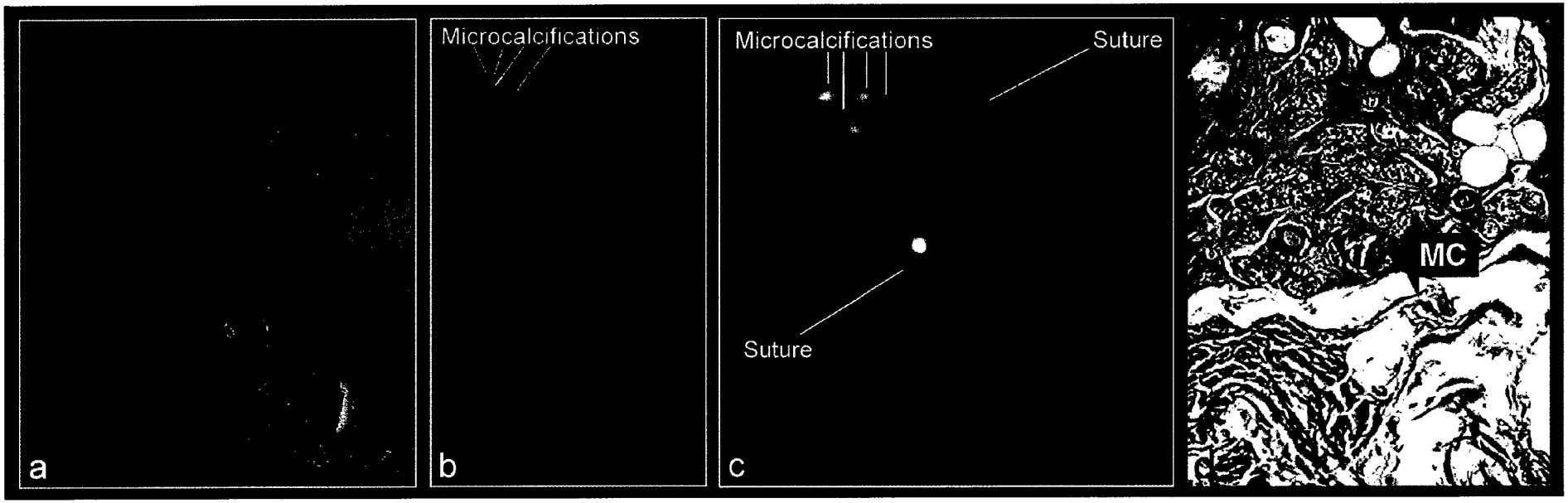

Figure 4

Fig. 4

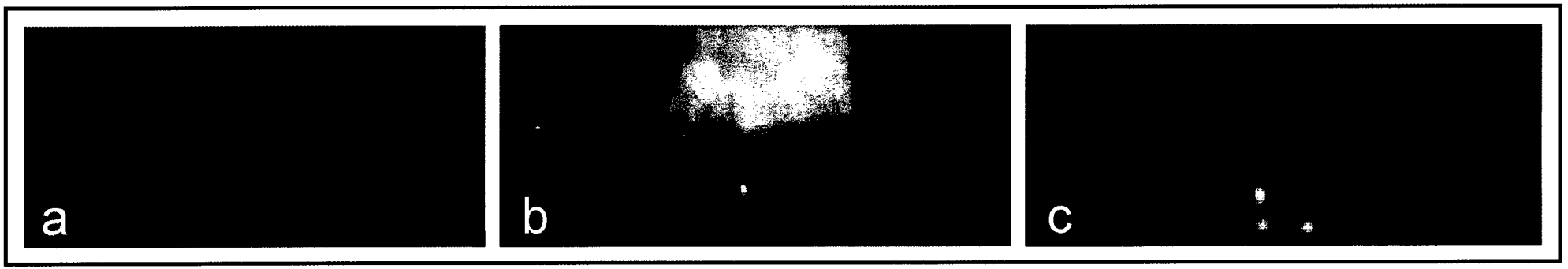

Figure 5

Fig. 5

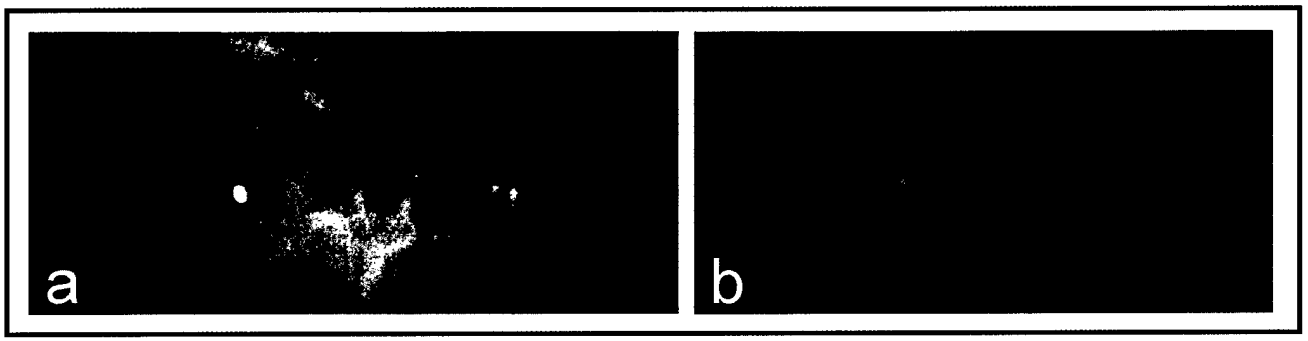

Figure 6

Fig. 6

Figure 7

Fig. 7

will provide a solid foundation for the establishment of the HELS method as a potentially viable noise diagnostic tool. [Work sponsored by NSF and Ford Motor Company.]

Appendix D

11:00

2aSA7. Determination of the optimal number of expansion terms in the HELS method. Byoung-Duk Lim (Dept. of Mech. Eng., Yeungnam Univ., 214-1 Dae-dong, Gyongsan, Kyungbuk, 712-749, Korea) and Sean F. Wu (Wayne State Univ., Detroit, MI 48202)

The Helmholtz equation least-square (HELS) method has been proven to be an efficient way of reconstructing acoustic radiation from a vibrating structure [Wu, J. Acoust. Soc. Am. **107**, 2511–2522 (2000)]. In this method, the optimal number of expansion terms is determined by a heuristic method of searching the minimum–norm errors of the reconstructed acoustic pressures with respect to the measured data. While this approach works, it is time consuming. In this paper, a new method of *a priori* determination of the optimal number of expansions is developed based on the eigenvalue analysis of the measured information. Assuming a Gaussian white measurement noise, the hypothesis of equal noise eigenvalues is tested based on the statistical properties of the eigenvalues. This hypothesis test yields an upper bound of the optimal number of expansions in general. Also developed is a method for testing the correlation coefficients after eliminating some principal components, which gives a lower bound of the optimum number of expansions. Since the curve of minimum–norm errors in the previous work shows local minima when the number of terms is squares of the integer, the range produced by the present method leads to only a few candidates for the optimal number of expansions. Examples of reconstructing the radiated acoustic pressure field from a vehicle front end using the optimal number of expansion terms thus obtained are demonstrated in parallel with the results of the *a posteriori* method discussed by Wu. [Work supported by NSF.]

11:15

2aSA8. Vibro-acoustography of small spheres. Shigao Chen, Mostafa Fatemi, and James F. Greenleaf (Dept. of Physiol. and Biophys., Mayo Clinic, Rochester, MN 55905, chen.shigao@mayo.edu)

Vibro-acoustography is a method for imaging the acoustic energy emitted from objects in response to an oscillatory radiation force produced by two interfering focused beams of ultrasound [M. Fatemi and J. F. Greenleaf, Science **280**, 82–85 (1998)]. To facilitate quantitative study, a model is presented that describes the behavior of an elastic sphere in two plane ultrasound waves of slightly different frequencies. The vibrating velocity and the resulting acoustic emission of the sphere at the difference frequency are derived from the radiation force and the impedance of the sphere. For small steel spheres in water, the velocity and emission are predicted to have a simple relationship with the difference frequency and the size of the sphere. Experiments on small stainless steel spheres of different size are carried out for a number of difference frequencies, with a laser interferometer to measure the velocity of the sphere and a calibrated hydrophone to measure the acoustic emission from the sphere. The experimental results fit the model description well. This means that vibro-acoustography may be useful in quantitative measurement.

11:30

2aSA9. Backscattering enhancements associated with antisymmetric Lamb waves on circular plates in water: Observations and imaging of the plate surface using acoustic holography. Brian T. Hefner and Philip L. Marston (Phys. Dept., Washington State Univ., Pullman, WA 99164, bhefner@mail.wsu.edu)

When a tilted circular plate is illuminated with high-frequency sound in water, significant enhancements occur when the angle of incidence corresponds to a Lamb wave coupling angle. Previously, scattering associated with the lowest-order symmetric Lamb wave, s_0, was studied using acoustic holography and modeled using quantitative ray methods [B. T. Hefner and P. L. Marston, J. Acoust. Soc. Am. **107**, 2847 (2000)]. The present investigation focuses on backscattering associated with the antisymmetric Lamb waves. Above the cutoff frequency of the first-order antisymmetric wave, a_1, enhancements are observed which are associated with both the a_1 wave and the a_0 wave. For these enhancements, however, mode conversion between these modes plays a significant role. To examine the mode conversion and to identify the scattering mechanisms, acoustic holography was used to image the plate surface when the plate is ensonified at the a_1 wave coupling angle. From the imaged wave field, the enhancement at this angle involves a wave which moves around the circumference of the plate: a "whispering gallery" mode involving the a_1 wave or a flexural edge wave. Both of these possibilities are considered as well as a possible scattering mechanism at the a_0 wave coupling angle. [Work supported by the Office of Naval Research.]

11:45

2aSA10. Diagnostics of vibration and noise via Fourier transforms: A new approach. Leonid M. Gelman (Dept. of Nondestructive Testing, Natl. Tech. Univ. of Ukraine, 37, Peremogy Pr., Kiev, 252056, Ukraine), Ivan V. Petrunin (Natl. Tech. Univ. of Ukraine, Kiev, 252056, Ukraine), and Vladimir T. Shirkov ("Motor-Sich" Co., Zaporozh'e, 01202, Ukraine)

A new general optimal approach and new diagnostic features are proposed, for those cases where one- and multidimensional Fourier transforms are used for diagnostics of vibration and noise. For the forced oscillation vibroacoustical diagnostics method with Gaussian excitation, the optimal nonlinear transformation of the proposed features is received. It was shown (1) The power spectral density is optimal transformation for considered diagnostics only for specific situations; (2) The phase spectrum is not optimal transformation for considered diagnostics; and (3) The proposed approach provides the increment of diagnostics effectiveness in contrast with usage of power spectral density. This is in contrast to most applications concerning diagnostics of vibration and noise, where power spectral density is used.

Appendix E

Title/Referral Page

No Page Limit

Proposal title (up to 160 characters)

DEVELOPMENT OF VIBRO-ACOUSTOGRAPHY FOR IN-VIVO DETECTION OF BREAST MICROCALCIFICATIONS

PI's full name (first, middle initial, last)

MOSTAFA FATEMI

Award mechanism

IDEA

PI's phone number, fax number, and e-mail address

TELEPHONE: 507-284-0608
FAX: 507-266-0608
E-MAIL: FATEMI.MOSTAFA@MAYO.EDU

Organization name and location (including city, state, zip or postal code, and country)

MAYO MEDICAL CENTER
200 FIRST STREET SW
ROCHESTER, MN 55905 USA

Name of administrative representative authorized to conduct negotiations

BONNIE A. EDWARDS

Phone number, fax number, and e-mail address of administrative representative authorized to conduct negotiations

TELEPHONE: 507-284-4715
FAX: 507-284-1772
E-MAIL ADDRESS: EDWARDS.BONNIE@MAYO.EDU

TECHNICAL ABSTRACT

Development of Vibro-acoustography for In-vivo Detection of Breast Microcalcifications
Mostafa Fatemi, Ph.D., Idea Award Recipient

Background: X-ray mammography is the only imaging modality used today for detection of breast microcalcifications. This important tool, however, is ionizing, and its sensitivity is greatly reduced in dense breasts. It is estimated that half of the women in the United States have fibrocystic breasts, and many of them have very dense breast tissue. For this group, the failure rate of x-ray mammography in detection of calcification can be as high as 15-25%. Vibro-acoustography (VA) is a novel noninvasive imaging technique that uses ultrasound in a fundamentally new way. In this method, the object is vibrated by the radiation force of ultrasound at a low (kHz range) frequency; and the resulting acoustic emission field is detected by a hydrophone and used to produce images that are related to the mechanical properties (such as relative hardness) of the object. Microcalcifications that are much harder than soft tissue will appear much brighter than the surrounding tissue in VA images.

Because ultrasound can penetrate radiologically-dense tissue without much difficulty, breast density does not seem to be a problem in VA imaging. Another feature of this method is that it can be tuned to operate as a "point detector," with increased sensitivity to small-size objects. This feature makes VA particularly suitable for detection of breast microcalcifications. We have shown that VA can detect microcalcifications as small as 110 μm-diameter in excised human breast tissue.

Objective/Hypothesis: We hypothesize that VA can be used for in-vivo breast imaging. The purpose of this research is to test the capability of VA in detecting microcalcifications in human breast.

Specific Aims: **(1)** Develop an experimental VA system for in-vivo breast scanning. This aim includes (a) design a new scanning system for in-vivo breast imaging; (b) measure system parameters, such as peak ultrasound intensity and spatial resolution; (c) evaluate/assure ultrasound exposure safety. **(2)** Develop a method for producing VA and mammography image pairs that are geometrically similar and, hence, can be correlated. **(3)** In-vivo breast imaging, including (a) recruiting patients; (b) evaluating patients; (c) conducting x-ray mammography; (d) detecting microcalcifications in mammograms; (e) scanning breasts by the VA system developed in Aim1. **(4)** Evaluate the performance of VA in detecting microcalcifications, including: (a) detecting microcalcifications in VA images; (b) correlating corresponding VA and x-ray images; (c) determining the success rate of VA method in detecting microcalcifications based on the microcalcifications found in the corresponding x-ray.

Study Design: Twenty Volunteers with proven microcalcifications in their breasts will be recruited for the study. X-ray or stereo mammography will be used as the gold standard to verify and localize microcalcifications. A prototype VA system will be designed and used to scan the breast (at an orientation similar to that of x-ray). The resulting image will be compared with the corresponding mammograms. The success rate of VA will be determined by correlating the microcalcifications that are detected by VA with those identified in the corresponding mammograms.

Relevance: Successful in-vivo detection of microcalcifications will open the way for clinical use of vibro-acoustography as a noninvasive alternative to mammography. This imaging technique may be useful both as a diagnostic and screening modality. This device could be a particularly valuable tool for patients with very dense breasts where mammographic detection of early cancer is limited. The lack of ionizing radiation would be of benefit to all patients, but especially very young or pregnant women.

AA

Appendix F

Form Approved Through 2/28/01
OMB No. 0925-0001

Department of Health and Human Services
Public Health Service

Grant Application

Follow instructions carefully.
Do not exceed character length restrictions indicated on sample.

LEAVE BLANK—FOR PHS USE ONLY.

Type	Activity	Number
Review Group		Formerly
Council/Board *(Month, Year)*		Date Received

1. TITLE OF PROJECT
Vibro-Acoustography System with Contact Array Probe.

2. RESPONSE TO SPECIFIC REQUEST FOR APPLICATIONS OR PROGRAM ANNOUNCEMENT [ ] NO [X] YES *(If "Yes," state number and title)*
Number: PAR-01-057 Title: Technology Development for Biomedical Applications: Phased Innovation Award (R21/R33)

3. PRINCIPAL INVESTIGATOR/PROGRAM DIRECTOR New Investigator [X] YES

3a. NAME *(Last, first, middle)*	3b. DEGREE(S)	3c. SOCIAL SECURITY NO.
Fatemi, Mostafa, A	PhD	**Provide on Form Page KK.**

3d. POSITION TITLE
Assistant Professor

3e. MAILING ADDRESS *(Street, city, state, zip code)*
Mayo Clinic Rochester
200 First Street S.W.
Rochester , MN 55905

3f. DEPARTMENT, SERVICE, LABORATORY, OR EQUIVALENT
Dept. of Physiology & Biophys.

3g. MAJOR SUBDIVISION
Div. of Physiology & Biophys.

3h. TELEPHONE AND FAX *(Area code, number and extension)*
TEL: (507) 284-0608
FAX: (507) 284-1632

E-MAIL ADDRESS: fatemi.mostafa@mayo.edu

4. HUMAN SUBJECTS	4a. If "Yes," Exemption no. or IRB approval date	4b. Assurance of compliance no.	5. VERTEBRATE ANIMALS	5a. If "Yes," IACUC approval date	5b. Animal welfare assurance no.
[X] No [ ] Yes	[ ] Full IRB or [ ] Expedited Review		[X] No [ ] Yes		

6. DATES OF PROPOSED PERIOD OF SUPPORT *(month, day, year—MM/DD/YY)*		7. COSTS REQUESTED FOR INITIAL BUDGET PERIOD		8. COSTS REQUESTED FOR PROPOSED PERIOD OF SUPPORT	
From	Through	7a. Direct Costs ($)	7b. Total Costs ($)	8a. Direct Costs ($)	8b. Total Costs ($)
04/01/2002	03/31/2006	$103,647	$153,916	$1,603,647	$2,055,116

9. APPLICANT ORGANIZATION
Name: Mayo Clinic Rochester
Address: 200 First Street Southwest
Rochester , MN 55905

10. TYPE OF ORGANIZATION
Public: → [ ] Federal [ ] State [ ] Local
Private: → [X] Private Nonprofit
Forprofit: → [ ] General [ ] Small Business

11. ORGANIZATIONAL COMPONENT CODE 60

12. ENTITY IDENTIFICATION NUMBER
1416011702A1
DUNS NO. *(if available)*
00-647-1700

Congressional District: 01

13. ADMINISTRATIVE OFFICIAL TO BE NOTIFIED IF AWARD IS MADE
Name: Bonnie A. Edwards
Title: Assistant Treasurer
Address: Mayo Clinic Rochester
200 First Street Southwest
Rochester , MN 55905
Telephone: (507) 284-1864
Fax: (507) 284-1772
E-mail: researchadmin@mayo.edu

14. OFFICIAL SIGNING FOR APPLICANT ORGANIZATION
Name: Bonnie A. Edwards
Title: Assistant Treasurer
Address: Mayo Clinic Rochester
200 First Street Southwest
Rochester , MN 55905
Telephone: (507) 284-1864
Fax: (507) 284-1772
E-mail: edwards.bonnie@mayo.edu

15. PRINCIPAL INVESTIGATOR/PROGRAM DIRECTOR ASSURANCE: I certify that the statements herein are true, complete and accurate to the best of my knowledge. I am aware that any false, fictitious, or fraudulent statements or claims may subject me to criminal, civil, or administrative penalties. I agree to accept responsibility for the scientific conduct of the project and to provide the required progress reports if a grant is awarded as a result of this application.

SIGNATURE OF PI / PD NAMED IN 3a. *(In ink. "Per" signature not acceptable.)* Mostafa Fatemi — DATE 5/31/01

16. APPLICANT ORGANIZATION CERTIFICATION AND ACCEPTANCE: I certify that the statements herein are true, complete and accurate to the best of my knowledge, and accept the obligation to comply with Public Health Service terms and conditions if a grant is awarded as a result of this application. I am aware that any false, fictitious, or fraudulent statements or claims may subject me to criminal, civil, or administrative penalties.

SIGNATURE OF OFFICIAL NAMED IN 14. *(In ink. "Per" signature not acceptable.)* Bonnie A Edwards — DATE 5/31/01

DESCRIPTION: State the application's broad, long-term objectives and specific aims, making reference to the health relatedness of the project. Describe concisely the research design and methods for achieving these goals. Avoid summaries of past accomplishments and the use of the first person. This abstract is meant to serve as a succinct and accurate description of the proposed work when separated from the application. If the application is funded, this description, as is, will become public information. Therefore, do not include proprietary/confidential information. **DO NOT EXCEED THE SPACE PROVIDED.**

Viscoelastic properties of tissues are closely related to the tissue state and pathology.

Vibro-acoustography (**VA**) is new imaging method developed in our laboratory that produces a display of the dynamic response of tissue to a vibrating force at a selected low frequency (kHz range). Such images may be used for evaluation of tissue pathology.

A vibro-acoustography system uses the radiation force of ultrasound to produce a highly concentrated oscillating force that vibrates the object at each point. Object response is recorded by a hydrophone and used to produce the image. The result is a speckle-free, transverse view, representing the dynamic response of the object to the vibrating force. In preliminary *in vitro* experiments, we have shown that vibro-acoustography can be used to image hard materials such as calcifications inside human arteries, very small particles such as micron-size microcalcifications in human breast tissue, and lesions in liver. VA can also be used to image and evaluate the integrity of prosthetic heart valves.

The purpose of this proposal is to develop a vibro-acoustography system with a contact probe for *in vivo* applications. The goal of this research will be achieved in two phases. The first phase consists of computer simulation of the system. The second phase focuses on system implementation. The aims of the first phase include: system design, modeling, and evaluating system performance. The aims of the second phase include design and construction of the ultrasound probe, design and construction of system electronics (transmitter, receiver, and monitor), and evaluating and optimizing system performance. Successful completion of this research will result in a new class of noninvasive imaging and tissue evaluation device, which will provide information about the mechanical properties of tissue that are not available from other imaging modalities.

PERFORMANCE SITE(S) *(organization, city, state)*

Mayo Foundation
Rochester, MN 55905

KEY PERSONNEL. See instructions on Page 11. *Use continuation pages as needed* to provide the required information in the format shown below.

Name	Organization	Role on Project
Mostafa Fatemi, Ph.D.	Mayo Foundation	Principal Investigator
James F. Greenleaf, Ph.D.	Mayo Foundation	Co-Investigator
Azra Alizad, M.D.	Mayo Foundation	Co-Investigator
To Be Named	Mayo Foundation	Research Fellow
Richard L. Ehman, M.D.	Mayo Foundation	Consultant